2007-05

UNDERSTANDING CORONAL HEATING AND SOLAR WIND ACCELERATION: CASE FOR IN SITU NEAR-SUN MEASUREMENTS

D. J. McComas,[1] M. Velli,[2,3] W. S. Lewis,[1] L. W. Acton,[4] M. Balat-Pichelin,[5] V. Bothmer,[6] R. B. Dirling Jr.,[7] W. C. Feldman,[8] G. Gloeckler,[9] S. R. Habbal,[10] D. M. Hassler,[11] I. Mann,[12] W. H. Matthaeus,[13] R. L. McNutt Jr.,[14] R. A. Mewaldt,[15] N. Murphy,[3] L. Ofman,[16] E. C. Sittler Jr.[17] C. W. Smith,[18] and T. H. Zurbuchen[19]

Received 5 January 2006; revised 18 August 2006; accepted 24 October 2006; published 17 March 2007.

[1] The solar wind has been measured directly from 0.3 AU outward, and the Sun's atmosphere has been imaged from the photosphere out through the corona. These observations have significantly advanced our understanding of the influence of the Sun's varying magnetic field on the structure and dynamics of the corona and the solar wind. However, how the corona is heated and accelerated to produce the solar wind remains a mystery. Answering these fundamental questions requires in situ observations near the Sun, from a few solar radii (R_S) out to $\sim$20 R_S, where the internal, magnetic, and turbulent energy in the coronal plasma is channeled into the bulk energy of the supersonic solar wind. A mission to make such observations has long been a top priority of the solar and space physics community. The recent Solar Probe study has proven that such a mission is technically feasible and can be accomplished within reasonable resources.

Citation: McComas, D. J., et al. (2007), Understanding coronal heating and solar wind acceleration: Case for in situ near-Sun measurements, *Rev. Geophys.*, *45*, RG1004, doi:10.1029/2006RG000195.

1. INTRODUCTION

[2] The Sun is a main sequence star near the midpoint of its 10 billion year life span. Energy released by the fusion of hydrogen nuclei in its core slowly radiates through the solar interior until, about two thirds of the way from the Sun's center, radiative transfer is replaced by convection. The churning of the plasma in this region, the convective zone, powers a dynamo that generates the Sun's intense magnetic field, whose emergence through the *photosphere*, the solar "surface" seen in visible light, creates sunspots and sculpts the lower regions of the Sun's atmosphere into a dramatic and ever-changing architecture of filaments, loops, and arcades observable at ultraviolet and X-ray wavelengths. The magnetic field also structures the Sun's upper atmosphere or *corona*, forming both magnetically closed regions that can extend several solar radii into space and magnetically open regions known as *coronal holes*. The corona expands, in the form of a hot, magnetized stellar wind, to the very edge of the heliosphere, where, highly rarified, it encounters the plasma, neutral gas, and cosmic dust of the interstellar medium.

[1]Space Science and Engineering Division, Southwest Research Institute, San Antonio, Texas, USA.
[2]Dipartimento di Astronomia e Scienza del Spazio, Università degli Studi di Firenze, Florence, Italy.
[3]Jet Propulsion Laboratory, Pasadena, California, USA.
[4]Department of Physics, Montana State University, Bozeman, Montana, USA.
[5]Processes, Materials and Solar Energy, CNRS, Font-Romeu, France.
[6]Institut für Astrophysik, Georg-August-Universität Göttingen, Göttingen, Germany.
[7]Science Applications International Corporation, Fountain Valley, California, USA.
[8]Los Alamos National Laboratory, Los Alamos, New Mexico, USA.
[9]Department of Physics, University of Maryland, College Park, Maryland, USA.
[10]Institute for Astronomy, University of Hawaii at Manoa, Honolulu, USA.
[11]Space Studies Department, Southwest Research Institute, Boulder, Colorado, USA.
[12]Department of Earth and Planetary Sciences, Kobe University, Kobe, Japan.
[13]Bartol Research Institute, University of Delaware, Newark, Delaware, USA.
[14]Johns Hopkins University Applied Physics Laboratory, Laurel, Maryland, USA.
[15]Space Radiation Laboratory, California Institute of Technology, Pasadena, California, USA.
[16]Physics Department, Catholic University of America, Washington, D. C., USA.
[17]NASA Goddard Space Flight Center, Greenbelt, Maryland, USA.
[18]Department of Earth, Oceans and Space, University of New Hampshire, Durham, New Hampshire, USA.
[19]Department of Atmospheric, Oceanic, and Space Science, University of Michigan, Ann Arbor, Michigan, USA.

8755-1209/07/2006RG000195$15.00
Paper number 2006RG000195

[3] The discovery that the corona is many hundreds of times hotter than the photosphere and the development, and subsequent observational confirmation, of the theory of the corona's supersonic expansion into interplanetary space were among the fundamental advances in solar physics made during the last century. The discovery of the corona's million-degree temperature resulted from Bernard Lyot's invention, in 1930, of the coronagraph, which allowed scientists to perform spectroscopic studies to identify coronal emission lines and to measure their widths. The startling result of these studies, that elements such as iron were highly ionized, could only be explained if the temperature of the corona was far greater than the 6000 K temperature of the photosphere. While some early studies indicated coronal temperatures of several hundred thousand degrees, by the end of the 1950s, coronal temperatures averaging $\sim 2.4 \times 10^6$ K had been established, based on the analysis of emission line widths and brightness gradients [*Billings*, 1959] (on the history of the determination of coronal temperature, see *Noci* [2002]).

[4] *Biermann* [1951] (and subsequent papers) demonstrated that the acceleration of comet tails away from the Sun was caused not, as was commonly believed, by radiation pressure but by "solar corpuscular radiation," plasma flowing in all directions away from the Sun. This insight, together with Sydney Chapman's observation that Earth is immersed in the Sun's rarefied outer atmosphere (which Chapman believed to be static), led E. N. Parker to develop the theory of a supersonically expanding corona. Published in 1958 over the objections of the referees and highly controversial at the time [*Parker*, 1997], the theory of the "*solar wind*," the term Parker coined to describe the Sun's hydrodynamically expanding corona, was confirmed within just a few years by plasma measurements from the Soviet Luna and Venera spacecraft and America's Explorer 10 and Mariner 2 (on the history of the solar wind concept, see *Parker* [1997, and references therein]).

[5] The confirmation of Parker's theory did not, however, reveal how particles in the corona are accelerated to form the solar wind or where in the near-Sun environment the acceleration occurs. Nor did the observational determination of unexpectedly high coronal temperatures yield insight into the processes by which energy is transferred from the photosphere to the corona and dissipated to heat the corona. Explaining these two related phenomena, the high-temperature corona and its acceleration to form a supersonic stellar wind, has remained a major focus of solar and heliospheric physics research for the past half century.

[6] Although the twin mysteries of coronal heating and solar wind acceleration remain unsolved, remote-sensing observations from space-based platforms such as Yohkoh [*Ogawara et al.*, 1991], Solar and Heliospheric Observatory (SOHO) [*Domingo et al.*, 1995] and Transition Region and Coronal Explorer (TRACE) [*Schrijver et al.*, 1999] as well as from ground-based observatories, together with in situ measurements by Helios [*Schwenn and Marsch*, 1990], IMP [*Paularena and King*, 1999], Ulysses [*Balogh et al.*, 2001], Wind [*Ogilvie and Desch*, 1997], and ACE [*Stone et al.*, 1998], have significantly increased our knowledge and understanding of both phenomena. As the temporal and spatial resolution of instrumentation has increased and sophisticated computational models have been developed, the fundamental role played by the Sun's magnetic field in shaping dynamical processes on all scales in the three-dimensional heliosphere throughout the solar activity cycle has become more apparent. Significant progress has been made in our knowledge of coronal structures, particularly of fine-scale structures such as *polar plumes*, *coronal bright points* [*Golub et al.*, 1974], and the Sun's "*magnetic carpet*" [*Schrijver et al.*, 1998]; and we have witnessed fundamental advances in our understanding of the nature of the solar wind, the association of its fast and slow components with specific coronal structures, and its variability with changing solar activity.

[7] Important early clues about the bimodal structure of the solar wind came from the Helios mission, the only mission to explore the inner heliosphere as close to the Sun as 0.3–0.7 AU. Helios demonstrated that properties such as solar wind speed, ion temperatures, and turbulence amplitude increase with distance from the heliospheric *current sheet* [*Schwenn and Marsch*, 1990; *Grappin et al.*, 1990]. In its two orbits about the Sun's poles, Ulysses has explored the three-dimensional structure of the solar wind as it changes over the course of a solar activity cycle (Figure 1) [*McComas et al.*, 2003]. Ulysses has shown that the fast solar wind, with a speed around 750 km s^{-1}, is the basic, quasi-steady outflow from the high-latitude solar corona during the minimum phase of the solar cycle and demonstrated that the fast wind originates from regions where the coronal electron temperature is relatively low (Figure 2) [*Geiss et al.*, 1995]. This inverse correlation between flow speed and coronal electron temperature poses a fundamental challenge to one of the basic tenets of the original theory of the solar wind, which assumed high coronal electron temperatures and consequent heat conduction as a basic driving mechanism. A further challenge to the original theory comes from SOHO measurements, which suggest that the open corona expands principally because of the very high, anisotropic temperatures of the coronal ions, with the minor species reaching temperatures of 10 MK at a few solar radii [*Li et al.*, 1998; *Kohl et al.*, 1998].

[8] Unlike the fast wind, which originates in coronal holes, the slow solar wind is confined to regions emanating from the magnetic activity belt. SOHO observations suggest that the slow wind flows in a bursty, intermittent fashion from the top of *helmet streamers* [*Sheeley et al.*, 1997], which were first seen to expand continuously, in X rays, by Yohkoh [*Uchida et al.*, 1992]. The organization into fast and slow components characterizes the solar wind around solar minimum. As the solar activity cycle progresses, however, Ulysses has shown that the simple bimodal structure gives way to a much more variable, but typically slower, solar wind at activity maximum, apparently originating not only from the much more sparse coronal hole regions and quiet Sun but also from coronal *active regions* [*Liewer et al.*, 2004; *Neugebauer et al.*, 2002]. To whatever

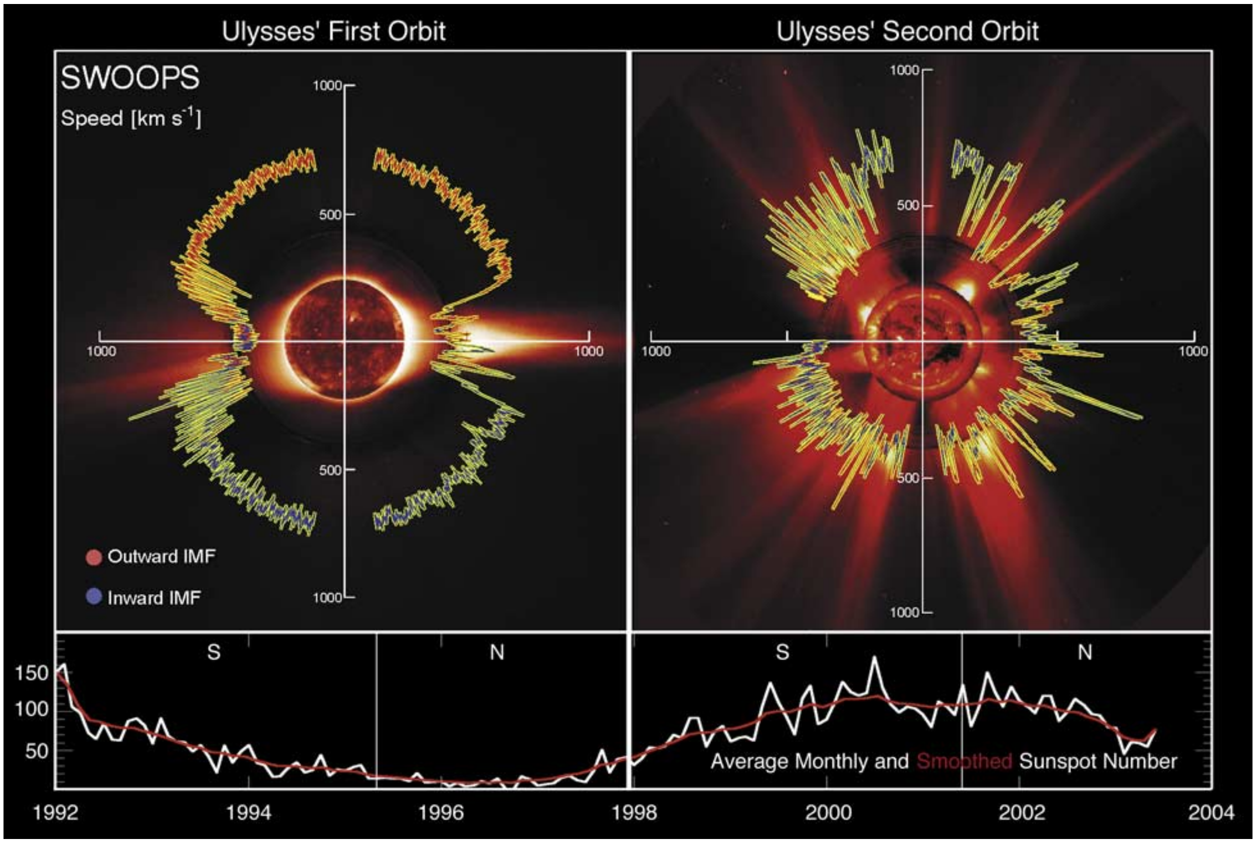

Figure 1. Plots of solar wind speed as a function of heliographic latitude illustrating the relation between the structure of the solar wind and coronal structure at (left) solar minimum and (right) solar maximum. (Ulysses Solar Wind Observations Over the Poles of the Sun (SWOOPS) solar wind data are superposed on composite solar images obtained with the SOHO EIT and LASCO C2 instruments and with the Mauna Loa K coronameter [*McComas et al.*, 2003].)

degree the various models of solar wind acceleration have succeeded in reproducing observations of the fast wind, still less success has been obtained in efforts to understand the acceleration of the slow wind.

[9] A third type of flow arises from large eruptions of coronal magnetic structures, known as *coronal mass ejections* (CMEs) [*Gosling et al.*, 1974; *Zhang and Low*, 2005]. Their initiation requires an entirely distinct mechanism from the slow and fast wind. One of the important developments in solar and heliospheric physics during the last 25 years is the recognition that shock waves driven by fast CMEs can relatively often accelerate particles to energies exceeding 1 GeV and that such shock-driven "gradual" energetic particle events are distinct from "impulsive" events associated with solar *flares* [*Reames*, 1999]. However, the identity of the seed particles and the physical conditions necessary for the acceleration of particles in gradual events are not known.

[10] It was recognized as early as 1958, at the very beginning of the space age, that solving the fundamental problems of coronal heating and solar wind acceleration requires sending a spacecraft into the inner heliosphere to make in situ measurements of the near-Sun particles-and-fields environment. Since then, a Solar Probe has been recommended consistently as a high priority mission in various National Research Council reports and NASA strategic planning documents and has been the subject of several NASA mission definition studies. The last and most extensive of these studies began in the spring of 2004 and concluded in the summer of 2005, with its final report being published in September 2005 [*NASA*, 2005a]. The Solar Probe Science and Technology Definition Team (STDT) that conducted this latest study reviewed the extensive literature on coronal heating and solar wind acceleration, with particular emphasis on recent observational and theoretical results. The STDT then defined a set of specific questions related to the sources of the solar wind and the coronal energy budget (Table 1, objectives 1 and 2) and the measurements needed to address them. Throughout their report the STDT was careful to discuss how specific near-Sun measurements will make it possible to test competing theories and models of coronal heating and solar wind acceleration and thus to solve these two fundamental problems of solar and heliospheric physics. (As a guide to the reader, Table 2 indicates the sections and paragraphs in this review where the relevance of the measurements to the various proposed heating and acceleration mechanisms is discussed.)

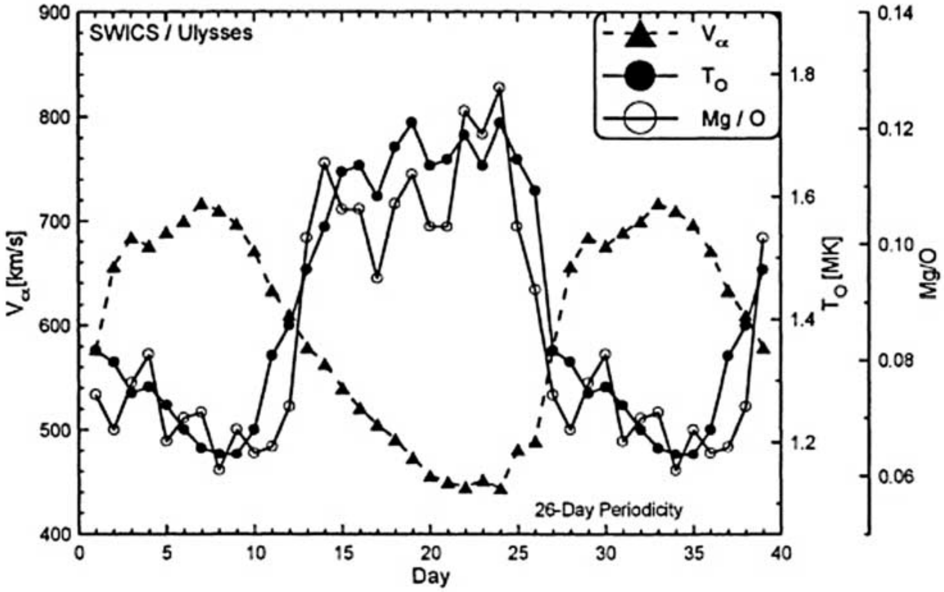

Figure 2. Alpha particle speed, freezing-in temperatures determined from O^{7+} to O^{6+} abundances, and magnesium to oxygen ratios as a function of time measured by Ulysses during a low-latitude crossing of alternating high- and low-speed streams. The anticorrelation of wind speed with electron temperature as determined from the freezing-in temperature is dramatic, calling into question the role of thermal electrons in driving the solar wind. Reprinted from *Geiss et al.* [1995, Figure 7], with kind permission of Springer Science and Business Media. Copyright 1995 Kluwer Academic Publishers.

[11] The team also reviewed the literature on the closely related topic of the acceleration and transport of solar energetic particles and, recognizing the opportunity afforded by proximity to the Sun to study cosmic dust in the near-Sun environment, reviewed the literature on the circumsolar dust cloud as well. On the basis of these reviews, the STDT established two additional science objectives (Table 1, objectives 3 and 4) that a Solar Probe mission will afford a unique opportunity to address.

[12] This article is adapted from the material presented in the science objectives chapter of the STDT report and is structured in terms of those objectives and associated questions.

2. SOURCES OF THE FAST AND SLOW SOLAR WIND

[13] In situ measurements of the solar wind by Ulysses and other spacecraft have confirmed the origin of fast wind streams in coronal holes and demonstrated the overall association of wind speed and coronal structure throughout the solar activity cycle (Figure 1) [*McComas et al.*, 2003].

TABLE 1. Scientific Objectives for a Solar Probe Mission

Objective	Question to Be Resolved
1. Determine the structure and dynamics of the magnetic fields at the sources of the solar wind	How does the magnetic field in the solar wind source regions connect to the photosphere and the heliosphere?
	How do the observed structures in the corona evolve into the solar wind?
	Is the source of the solar wind steady or intermittent?
2. Trace the flow of energy that heats the solar corona and accelerates the solar wind	How is energy from the lower solar atmosphere transferred to and dissipated in the corona?
	What coronal processes shape the nonequilibrium velocity distributions observed throughout the heliosphere?
	How do the processes in the corona affect the properties of the solar wind in the heliosphere?
3. Determine what mechanisms accelerate and transport energetic particles	What are the roles of shocks, reconnection, waves, and turbulence in the acceleration of energetic particles?
	What are the seed populations and physical conditions necessary for energetic particle acceleration?
	How are energetic particles transported radially and across latitudes from the corona to the heliosphere?
4. Explore dusty plasma phenomena and their influence on the solar wind and energetic particle formation	What is the dust environment of the inner heliosphere?
	What is the composition of dust-generated species near the Sun?
	What is the nature of dust-plasma interactions in the near-Sun environment?

TABLE 2. Relevance of Near-Sun Measurements to Proposed Coronal Heating and Solar Acceleration Mechanisms

Mechanisms	Sections/Paragraphs
Coronal heating by microflares and impulsive reconnection	2.3/27,29,30; 3.1/39,40; 3.3/52
Coronal heating and fast wind acceleration by Alfvénic turbulence	3.3/50,51
Coronal heating and fast wind acceleration by kinetic Alfvén waves	3.2/46
Coronal heating by phase mixing and resonance absorption	3.1/38; 3.2/43,44,45
Coronal heating by velocity filtration/electron beams	3.1/42
Fast solar wind and coronal structures	2.2/21,22; 2.3/27,29
Slow solar wind acceleration by reconnection/plasmoid ejection	2.2/23,24; 2.3/28,29; 3.3/52

However, while the properties of the fast and slow wind in interplanetary space are well established, their source regions have been explored only via remote sensing observations, which have revealed that the solar corona, even at solar minimum, displays a rich variety of dynamic magnetized structures over a wide range of temporal and spatial scales. Determining how these dynamic structures merge, in time and space, to yield the wind measured in interplanetary space cannot be achieved with remote sensing alone but requires a combination of remote sensing observations (e.g., of the polar photospheric magnetic fields) and in situ particles-and-fields measurements within a few R_S of the Sun.

2.1. Magnetic Field in the Solar Wind Source Regions

[14] The geometry of the magnetic field expansion in the inner corona, from the photosphere out to a few solar radii, plays a fundamental role in determining the density distribution and solar wind speeds in solar wind models, as the field lines define the flow tubes along which mass and energy flux are conserved. Close to the Sun, Solar Ultraviolet Measurements of Emitted Radiation (SUMER) and Michelson Doppler Imager (MDI) observations from SOHO suggest that the source of the fast solar wind is associated with the strong supergranular network magnetic fields in coronal holes [*Hassler et al.*, 1999] (Figure 3), which rapidly fan out to fill the corona [*Tu et al.*, 2005]. Ulysses observations have shown that the radial magnetic field component measured in the fast wind is largely independent of latitude [*Smith et al.*, 2003] so that any latitudinal gradient in the average field at the coronal base must be washed out by transverse nonradial expansion closer to the Sun. This nonradial divergence of the magnetic field is a fundamental property of the corona [e.g., *Feldman et al.*, 1996] as it determines the areal expansion along flux tubes, which has been shown to be inversely correlated with the asymptotic solar wind speed [*Levine*, 1978; *Wang and Sheeley*, 1990]. It is thought that flux tube expansion is caused by the excess high-latitude magnetic pressure, and models suggest that it occurs out to radial distances >10 R_S. On the basis of Ulysses data the magnitude of the average polar magnetic field has been estimated to be 6 G at solar minimum, although values up to 15 G in the photosphere cannot be ruled out. At present, there are no direct measurements of the polar magnetic field below 1.5 AU [*Sittler and Guhathakurta*, 1999, 2002]. Relating the mass and energy flux of the high-speed solar wind to the conditions at the base of the corona requires in situ measurement of the radial magnetic field and simultaneous remote sensing of the polar photospheric field. Such measurements will allow a complete description of magnetic field and solar wind expansion free from unknown parameters and provide both a test of existing models of coronal structure and rigorous constraints on future coronal models.

[15] The *magnetic network* in the quiet Sun looks remarkably similar to the network in coronal holes in spectral lines formed at lower, *transition region* temperatures, while it is harder to distinguish in lines formed at 10^6 K. If a similar coronal heating mechanism is at work in both the quiet Sun and coronal holes, any difference in their appearance is presumably related to the magnetic field topology, including, perhaps, its time dependence. The larger densities, apparently higher electron temperature, and different chemical composition of the quiet Sun would then be the result of a larger *filling factor* of closed magnetic field lines compared with those in coronal holes. While the imprint of

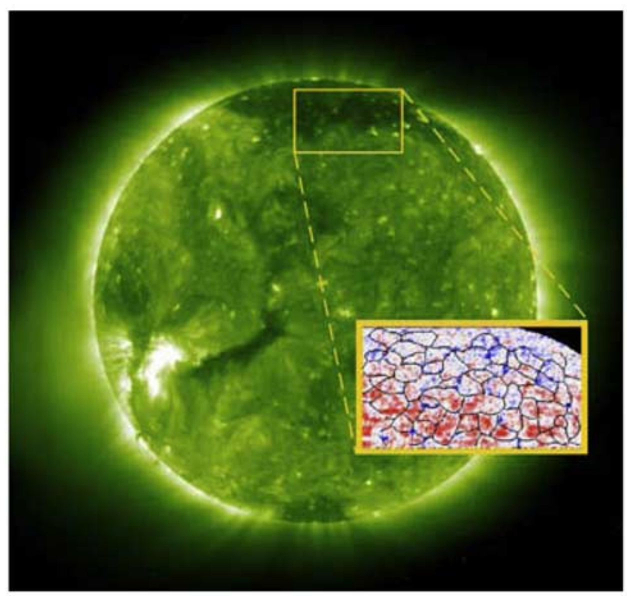

Figure 3. Polar coronal holes, such as that seen in this SOHO EIT image, which are the source of the fast solar wind. SUMER measurements of doppler-shifted coronal emission lines superposed on the magnetic network (inset) suggest that the high-speed outflow from coronal holes is associated with the chromospheric network [*Hassler et al.*, 1999]. Local measurements of such outflows will provide the data needed to test the hypothesis that the primary source region for the fast solar wind is in the magnetic network.

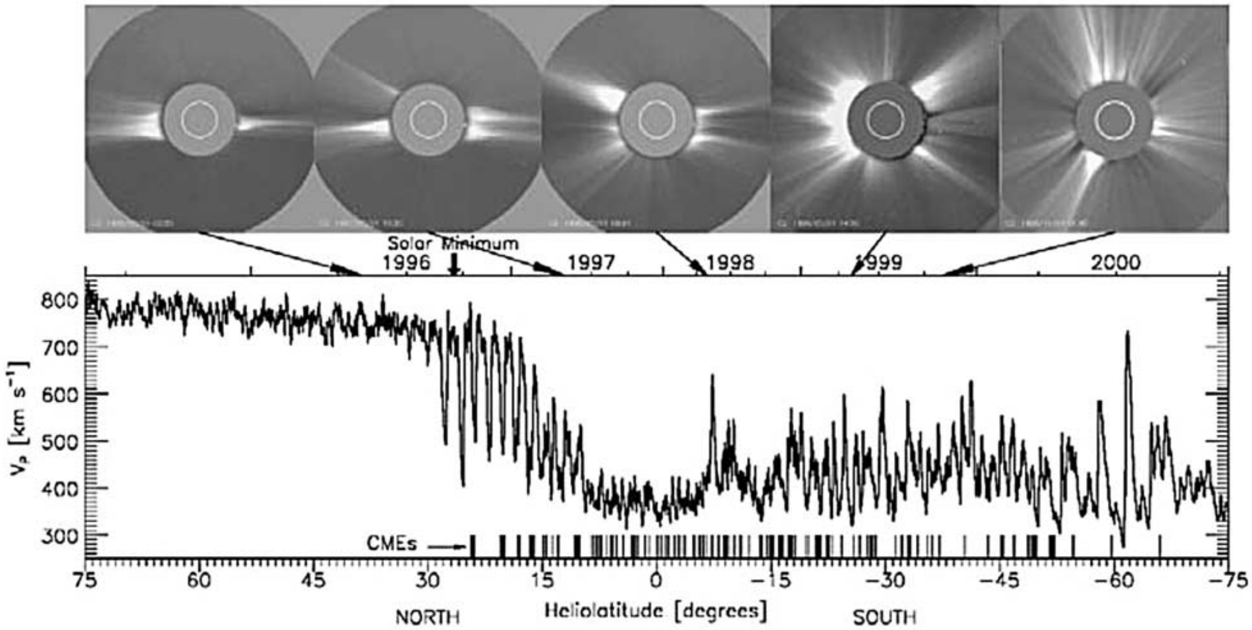

Figure 4. (top) SOHO LASCO C2 images showing the evolution of the streamer belt during the rising phase of solar cycle 23 and near solar maximum. With increasing activity, polar coronal holes shrink and streamers appear at higher and higher heliolatitudes. (bottom) In situ plasma measurements by Ulysses over the period September 1995 to October 2000 revealing the changing structure of the solar wind with increasing activity. The solar wind loses its orderly bimodal character and becomes a complicated mixture of fast flows from small coronal holes and transients embedded in a moderate to slow wind from all latitudes [*McComas et al.*, 2001].

coronal holes and equatorial helmet streamers is manifest in the solar wind in the form of fast and slow streams and embedded plasma sheets, the fate of the quiet Sun corona is unknown. Is the plasma in the quiet Sun confined by closed magnetic field lines, so that the fast wind is entirely of coronal hole origin? Or is there a mass loss from the quiet Sun as well, and if so, what is its speed and how does it merge with the surrounding solar wind?

[16] The magnetic field in active regions above sunspots provides the strongest confinement of hot plasma in the corona and is seen as bright X-ray loops, which often end in cusp-like shapes at their summit. At greater heights, these develop into streamers, which at solar minimum are large and elongated and form a belt around the solar magnetic equator. Remote sensing observations by the SOHO Ultra-Violet Coronagraph Spectrometer (UVCS) of the EUV emission lines of minor ions, combined with multifluid models [*Ofman*, 2000], provide some clues about the source regions of the slow solar wind in *coronal streamers*, but the magnetic field topology in these regions and the role it plays in plasma outflow are unknown.

[17] The complexity of the coronal magnetic field structure increases with increasing activity during the solar cycle. At activity maximum, disk observations show the existence of very complicated loop structures, and images of the extended corona show streamers protruding from the solar surface not only in the equatorial regions but at all latitudes around the disk as well (Figure 4). It is not known, however, where the slow solar wind forms in and around streamers and whether specific magnetic signatures, such as embedded current sheets, are associated with its formation. Further, although studies of solar wind sources during solar maximum indicate a contribution to the wind from inside active regions as well, the topology of magnetic field lines within active regions that give rise to solar wind flow has not been established.

[18] In situ measurements of the solar wind over coronal holes, the quiet Sun, and the active solar corona at distances between 9 and 4 R_S and under both quiet and active conditions are needed to trace the origin of the fast and slow wind and to correlate the flow speed with closed/open magnetic field line topologies, as measured by photospheric field measurements and determined indirectly through the in situ measurement of such parameters as electron and energetic particle bidirectional streaming. At present, relating the solar wind to the coronal magnetic structures in which it originates involves mapping the measured photospheric field out to some radius, generally, $\sim$2–3 R_S, and extrapolating the solar wind flow radially backward to this same radius, where a boundary condition, typically that the magnetic field be radial, is imposed [*Schatten et al.*, 1969; *Altschuler and Newkirk*, 1969]. In situ magnetic field measurements within a few R_S at low heliolatitudes would provide definitive ground truth for such mapping, while polar data would allow a better reconstruction of the magnetic field from the Sun into interplanetary space.

[19] In situ measurements of the heliospheric magnetic field suggest a global structure that is generally similar to that predicted by *Parker* [1958], with a spiral structure caused by the combination of solar wind expansion and solar rotation and a warped current sheet separating the northern and southern polarities. However, it has been proposed [*Jokipii and Kota*, 1989], but not confirmed observationally inside 1.9 AU, that photospheric motions of magnetic field lines at low frequencies over the poles produce strong and variable deviations from the Parker's prediction for the global field structure at high latitudes. The resulting large-amplitude interplanetary fluctuations would be responsible for large changes in the predicted drift of galactic cosmic rays into the heliosphere. Ulysses observations of the magnetic field orientation in corotating rarefaction regions also show large deviations from Parker's model [*Murphy et al.*, 2002; *Schwadron*, 2002]. Further evidence that the field deviates from the Parker model at large distances from the Sun came from the surprising detection by Ulysses of solar energetic particles at higher latitudes caused by shocks associated with cororating interaction regions (CIRs) formed at lower latitudes [*McKibben et al.*, 2001]. It has been suggested that the observed departures from the *Parker spiral* result in part from the rigid rotation of coronal holes, which implies efficient *reconnection* between the open coronal hole field lines and the quiet Sun and the resulting diffusion of open field lines across coronal hole boundaries [*Fisk*, 1996; *Fisk and Schwadron*, 2001]. In situ measurements of the magnetic field along a polar orbit spanning from a few AU down to 4 R_S would provide the data needed to test such theories of the heliospheric magnetic field.

2.2. Evolution of Coronal Structures Into the Solar Wind

[20] The outer solar atmosphere is structured by the magnetic field over a wide range of scales. Active regions and the quiet Sun display extended arcades and loops with thicknesses down to present observational resolution limits of 1000 km or less, merging into the helmet streamers observed over the activity belt in coronagraph images. White light and UV coronograph-spectroscopic observations show coronal holes to be far from featureless as well. Bright striations, or plumes, can be traced all the way from the solar surface out to 30 R_S (Figure 5).

[21] The relationship of plumes to the fast wind is poorly understood. They appear above X-ray bright points in the coronal holes and are denser by factors of 2 or more than the surrounding regions. UV lines in the plumes appear to be narrower (i.e., the plumes are cooler) than in the darker lanes separating them, while measurements of outflows suggest that the dark lanes are preferential outflow regions [*Teriaca et al.*, 2003]. Earlier measurements also revealed an apparent large *first ionization potential* (FIP) effect in plumes, thus excluding the possibility that they could be the source of the fast wind. However, more recent analyses using SOHO Coronal Diagnostic Spectrometer (CDS) data have shown that plumes do not have a significant FIP effect, contradicting the earlier observations [*Del Zanna et al.*, 2004]. Moreover, the scale height temperature in plumes seems to be too high to allow them to remain in static equilibrium [*Wilhelm et al.*, 1998], and dynamic wave activity, suggestive of acceleration mechanisms, has been observed in plumes by the SOHO Extreme ultraviolet Imaging Telescope (EIT) [*DeForest and Gurman*, 1998; *Ofman et al.*, 1999] and SOHO UVCS [*Ofman et al.*, 1997, 2000]. Finally, Doppler dimming measurements using SOHO SUMER in the height range 1.05–1.35 R_S have found outflow velocities in plumes of order 60 km s^{-1}, exceeding those in the interplume regions [*Gabriel et al.*, 2003].

[22] Fine-scale structures are observed in the fast wind as well as in coronal holes, including the so-called microstreams [*Neugebauer et al.*, 1995] and *pressure-balanced structures* [*Burlaga and Ogilvie*, 1970; *Thieme et al.*, 1989]. These are fluctuations in radial velocity that last about 16 hours in the spacecraft frame and have a magnitude of $\sim$50 km s^{-1}. Such structures may be a remnant of the original acceleration process or perhaps are the final result of the merging of plume and interplume regions. In order to clarify how microstreams form and evolve and to determine their relationship to coronal fine-scale structures will require both in situ measurement and imaging of coronal structures within polar coronal holes over a range of distances from 30 to 8 R_S. In situ measurement of the magnetic field and of the plasma velocity and full distribution function (solar wind density, temperature, and composition) would make it possible to identify individual flow tubes, while tomographic reconstruction of white light coronagraphic images [*Jackson et al.*, 2004] acquired during passage through the holes would provide information on the filling factor and geometrical distribution of plumes.

[23] The Large Angle and Spectrometric Coronagraph (LASCO) and UVCS telescopes on the SOHO mission have made important contributions to our knowledge of the origins of the slow solar wind streams around helmet streamers (Figure 6). Sequences of LASCO difference images obtained in 1996 (sunspot minimum) give the impression of a quasi-continuous outflow of material in "puffs" from the streamer belt [*Sheeley et al.*, 1997]. A quantitative analysis of moving features shows that they originate above the cusp of helmet streamers and move radially outward, with a typical speed of 150 km s^{-1} near 5 R_S, increasing to 300 km s^{-1} at 25 R_S (Figure 7). The average speed profile is consistent with an isothermal corona at the temperature T $\approx 1.1 \times 10^6$ K (SOHO UVCS measurements indicate a temperature 1.6×10^6 K in the streamer core, at activity minimum) and a critical point near 5 R_S. The ejection of material may be caused by loss of confinement due to pressure-driven instabilities as the heated plasma accumulates or to current-driven instabilities (tearing and or kink-type instabilities) in the sheared field of the streamer [*Endeve et al.*, 2005; *Rappazzo et al.*, 2005; *Einaudi et al.*, 1999]. *Sheeley et al.* [1997] conclude that the features they observe trace the wind motion like "leaves in the wind." It is not known, however, whether the ejection of material from streamers occurs in a continuous flow or

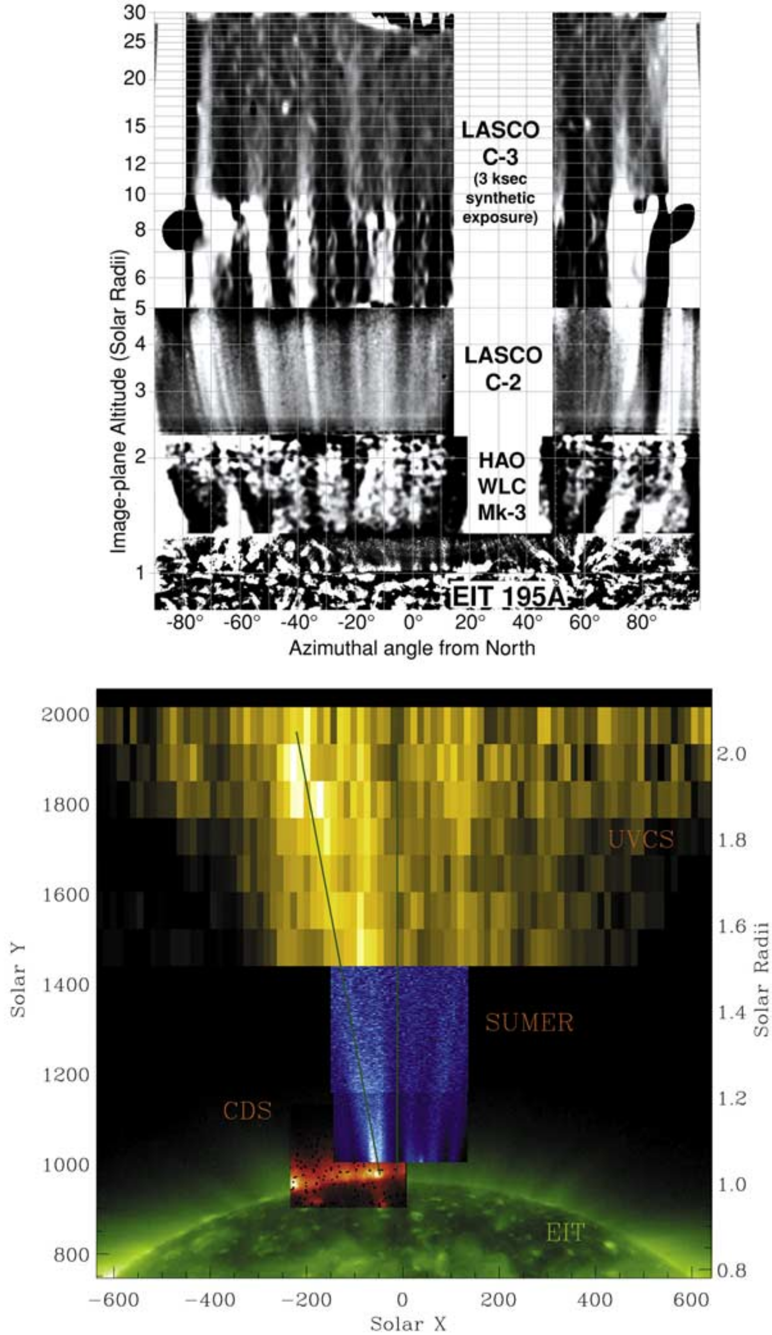

Figure 5. (top) A composite image showing the polar plumes and interplume regions from the surface out to a distance of 30 R_S [*DeForest et al.*, 2001]. (bottom) Composite showing detailed plume structure in the lower corona [*Teriaca et al.*, 2003]. It is unknown how polar coronal plumes are formed, how their density structures are maintained in the solar wind, and what their fate in the more distant heliosphere is, as in situ measurements from 1 AU are unable to identify them. Both images are reproduced by permission of the American Astronomical Society (AAS).

whether the puffs are, in fact, disconnecting plasmoids. In situ measurements across the paths of the ejecta are needed to answer this question and, in the case of plasmoids, to determine their magnetic field configuration as well as the magnetic morphology at the point of disconnection in the corona.

[24] Comparison of Galileo radio data with SOHO UVCS images clearly shows the association of the slow wind with *streamer stalks*, that is, with the regions above the cusps of helmet streamers that include the current sheet [*Habbal et al.*, 1997]. It is not known, however, whether there is a single current sheet that runs along the nearly equatorial strip of maximum brightness in the white corona, i.e., along the streamer belt (as surmised by *Wang et al.* [1997]) or whether there are a number of stalk/sheet structures of finite longitudinal extent. Nor is the structure of current sheets in

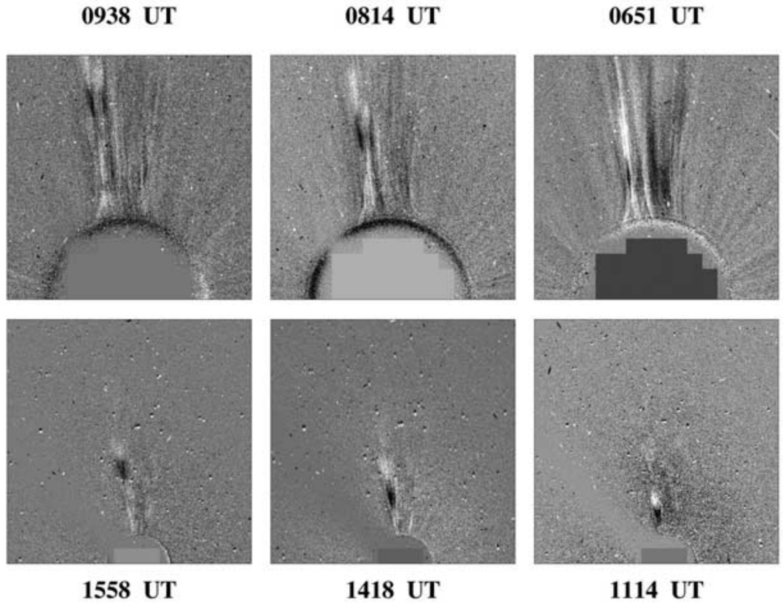

Figure 6. Difference images from SOHO LASCO showing the expulsion of material from the streamer belt [*Sheeley et al.*, 1997]. These images show how dynamic the release of mass from the magnetically confined corona may be. Reproduced by permission of the AAS.

streamer stalks known. Do they have a simple structure, or are they made up of multiple sheets in a more complex magnetic field morphology, as is suggested in part by SOHO UVCS measurements [*Noci et al.*, 1997] and in situ data acquired during multiple current sheet crossings [*Smith*, 2001]? These questions could be resolved through coronagraphic imaging of the plasma structures enveloping helmet streamers and through in situ measurements of the properties of the plasma and magnetic field in order to clarify the morphology of the magnetic field and nature of the current sheets.

[25] During periods of maximum activity the solar wind flow is much more variable and structured than the simple bimodal case found at solar minimum. The solar wind speed is typically lower, with the exception of very high speed CME-driven flows, and the source regions of the wind are more uncertain. The quasi-stationary (non-CME driven) flows appear to originate not only from coronal holes and their boundaries but also from active regions [*Liewer et al.*, 2004], which are associated with both the slower and moderately fast winds. The solar wind from active regions appears to be structured into substreams separated by distinctive structures such as magnetic holes [*Tsurutani et al.*, 2002], plasma sheets [*Crooker et al.*, 2004], or lower entropy regions [*Neugebauer et al.*, 2002]. Again, a combination of coronagraphic imaging and in situ measurements of the solar wind properties near the Sun is needed to characterize the evolution and structure of the wind from active regions.

2.3. Source of the Solar Wind: Steady or Intermittent?

[26] As observed in situ at large distances from the Sun, the solar wind appears as a continuous, if structured, plasma outflow. Its quasi-steady character may be a property of the outflow at the solar source. However, the apparently quasi-stationary wind may also result from a number of spatially limited, impulsive events that are distributed over smaller scales [*Neugebauer*, 1991; *Feldman et al.*, 1997].

[27] There is abundant evidence for the intermittent or "pulsed" [*Feldman et al.*, 1997] character of the high-speed wind: observations of microstreams and persistent beam-like features in the fast wind (Figure 8); interplanetary scintillation measurements of field-aligned density structures having a 10:1 radially aligned axial ratio and apparent field-aligned speeds ranging from $\sim$400 to $\sim$1280 km s^{-1} [*Coles et al.*, 1991; *Grall et al.*, 1996]; and remote sensing observations of the *chromosphere*, transition region, and corona revealing explosive, bursty phenomena (microflares) associated with magnetic activity over an extremely wide range of energy and timescales. *Feldman et al.* [1996, 1997] have interpreted the fine-scale structures observed in the fast wind as remnants of *spicules*, *macrospicules*, *X-ray jets*, and *H-alpha surges* and hypothesize that the fast wind results from the superposition of transient reconnection-generated jets. If this hypothesis is correct, then the heating of the corona would be accompanied by the annihilation of oppositely directed magnetic flux bundles clustered near the magnetic network, in turn leading to transient hard X-ray and gamma ray bursts, along with neutron production in the 1 to 10 MeV energy range, all of which would be detectable in near-Sun observations.

[28] For the slow solar wind, evidence in favor of an intermittent origin is even more abundant. As mentioned above, blobs of plasma appear to be lost by helmet streamer structures overlying active regions and various mechanisms have been proposed for this process. At solar maximum, an important and definitely intermittent solar wind component is present in the form of CMEs and the fine-scale structure

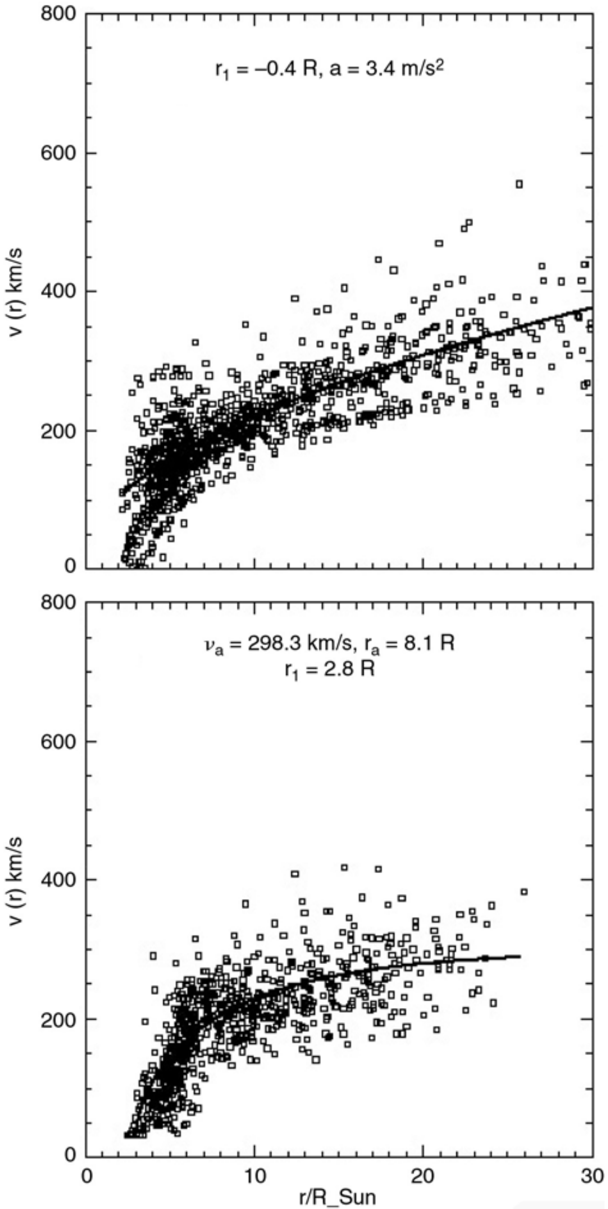

Figure 7. Scatterplots of the speed of density perturbations, or plasma puffs, as determined from difference images from the SOHO LASCO instrument, as a function of distance from the Sun, together with a best fit for the radial velocity profile [*Sheeley et al.*, 1997]. The plasma puffs serve as tracers of the slow solar wind, which experiences acceleration over a (top) more or (bottom) less extended radial distance from the Sun. Local measurements of densities and speeds within this full distance range can determine the contribution of plasmoids to the overall mass flux from the Sun. Reproduced by permission of the AAS.

of the solar wind from active regions suggests at least a spatially structured origin for the various flow streams. More generally, smaller CME-like events at all scales could contribute significantly to the solar wind throughout the activity cycle.

[29] Recent models of the solar wind [e.g., *Feldman et al.*, 1996, 1997; *Fisk*, 2003; *Schwadron and McComas*, 2003] require an intermittent, bursty origin for the solar wind, as the mass flux is lost by the reconnection of closed loops to open field lines. Loops may store plasma, accumulating energy and matter that will be injected in the solar wind. For a given energy flux, hotter loops contribute a larger mass flux, and therefore the asymptotic wind speed is lower. The inverse correlation of electron temperature and solar wind speed inferred from in situ observations [*Gloeckler et al.*, 2003] may thus be an intrinsic signature of the loops that are the source of solar wind. In this view, all solar wind material comes from plasma that was once confined in coronal loops and has therefore been injected into the wind via magnetic reconnection with open field lines [*McKenzie and Mullan*, 1997]. This view is also supported by in situ measurements of the abundance of elements with a low first ionization potential (FIP) bias, whose coronal accumulation can only occur in loops. FIP bias is close to two in the fast wind or high-latitude region and greater than three everywhere else [*Zurbuchen et al.*, 2002], evidence that the fast wind comes from small, short-lived loops, while slower wind may come from larger, longer-lived structures.

[30] Direct, in situ measurements of the structure of the solar wind, of the ion and electron distribution functions, and of elemental abundance variations close to the Sun are required to test these models. Key measurements include the electron distribution function and the flow speeds of minor ions in coronal holes, and, at lower heliographic latitudes, plasma composition on closed and open magnetic field lines. Continuous direct sampling of the plasma flow over a range of decreasing radial distances from the Sun would

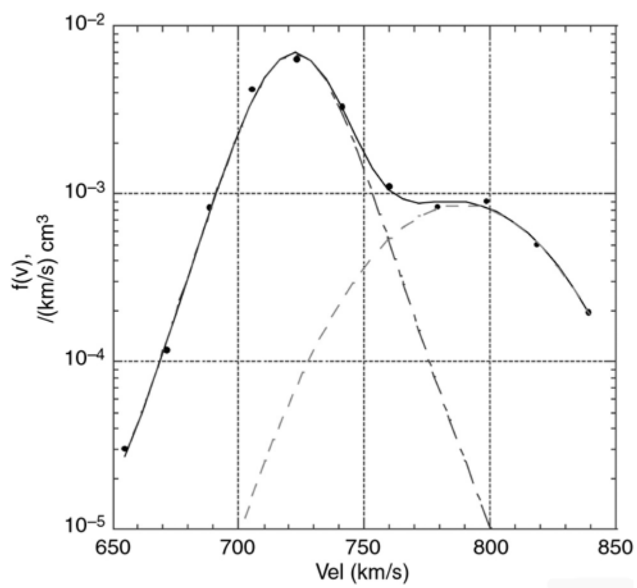

Figure 8. Two-beam model fit to the logarithm of phase space density for the Ulysses proton spectrum in the high-speed solar wind [*Goldstein et al.*, 2000]. A proton beam with a drift speed of about 50 km s^{-1}, i.e., the Alfvén speed, gives the best fit. Continuous plasma measurements inside 65 R_S can be used to determine where this beam forms and whether it is the direct remnant of the acceleration mechanism or is produced in situ by wave-particle interactions.

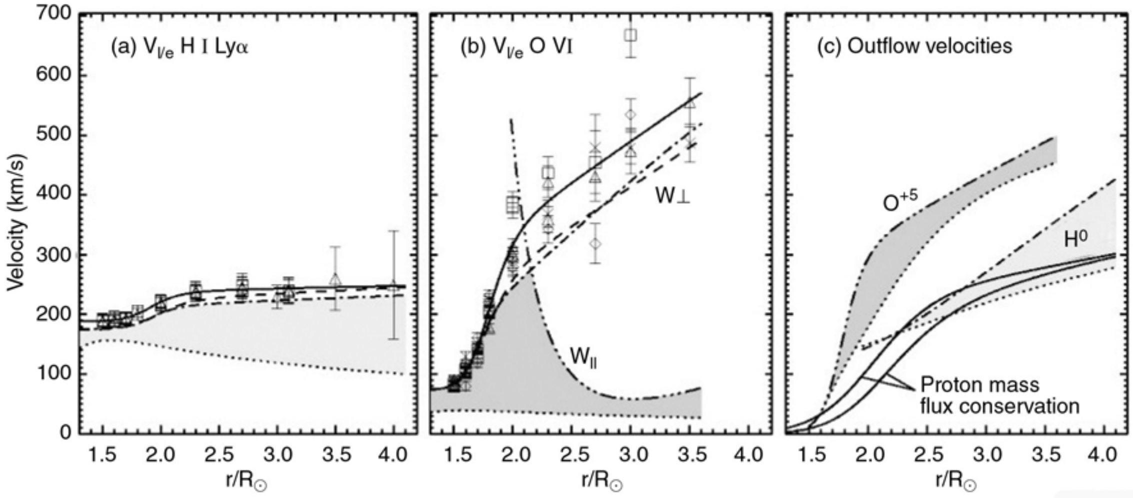

Figure 9. SOHO UVCS emission line width observations show anisotropic velocity distributions of neutral hydrogen (a proxy for protons) and $O^{5+}$and preferential acceleration of minor ions relative to the hydrogen atoms. Shaded areas indicate uncertainties due to thermal broadening. Preferential acceleration of the minor ions may result from ion cyclotron resonance or from wave-particle interactions involving nonlinear Alfvén waves [*Kohl et al.*, 1998]. Reproduced by permission of the AAS.

allow assessment of the spatial and temporal character of the filling factor of the fast solar wind. In situ measurements in the inner heliosphere would reveal how microstreams in the fast wind change and whether they merge with pressure-balanced or other density-enhanced plume-like structures. The observation of increased temporal variability in the solar wind near the Sun would be evidence of contributions to the outflow from multiple sources, such as bursty events or micro-CMEs.

3. FLOW OF ENERGY THAT HEATS THE CORONA AND ACCELERATES THE SOLAR WIND

[31] The solar corona loses energy in the form of radiation, heat conduction, waves, spicular mass injection and drainage to and from the photosphere, and the kinetic energy of the solar wind flow. It is estimated that the energy flux required to balance such losses from the corona varies from $e = 10^7$ erg cm^{-2} s^{-1} for active regions to $e = 5–8 \times 10^5$ erg cm^{-2} s^{-1} for coronal holes and streamer belt cusps [*Withbroe and Noyes*, 1977]. This energy must come from mechanical energy residing in photospheric convection, with the solar magnetic field acting both to channel and store this energy in the outer atmospheric layers. However, the mechanisms by which the energy is transferred and dissipated to generate the hot corona, solar wind, and heliosphere throughout the Sun's activity cycle remain one of the fundamental unanswered questions in solar and heliospheric physics.

[32] Remote-sensing measurements of the solar corona and in situ measurement of particle distribution functions in the fast and slow solar wind streams have shown that the heating process is correlated with magnetic structure, and at solar minimum, with the basic bimodal nature of the solar wind. SOHO UVCS observations using the Doppler dimming technique [*Li et al.*, 1998; *Kohl et al.*, 1998] (Figure 9) and interplanetary scintillation measurements [*Grall et al.*, 1996] (Figure 10) indicate that the high-speed solar wind is rapidly accelerated near the Sun, reaching speeds of the order of 600 km s^{-1} within 10 R_S. Observations of comet C/1996Y1 confirm a most probable speed of about 720 km s^{-1} for the solar wind at 6.8 R_S [*Raymond et al.*, 1998]. Such rapid acceleration appears to result from the extremely large and anisotropic effective temperatures in the lower corona that have been deduced from measurements by SOHO UVCS. These temperatures are much higher perpendicular to the magnetic field. The fast solar wind measured in situ shows what may be a relic of this anisotropy, which is smaller than that inferred from coronal observations, but persists in the distance range from 0.3 to 5 AU. Proton, alpha particle, and minor ion distribution functions in the fast wind also present a nonthermal beam-like component whose speed is comparable to the local *Alfvén speed*. All these properties suggest that Alfvén or *ion cyclotron waves* play a major role in coronal heating and solar wind acceleration. It is difficult, however, to separate remnant signatures of solar wind acceleration from in situ processes. Measurements close to the Sun are required to distinguish the effects of in situ processes and obtain a more direct measure of the acceleration mechanism(s).

[33] The different properties of the turbulence observed in the fast and slow solar wind are further evidence of the role played by turbulence and wave-particle interactions in coronal heating. Fast streams contain stronger fluctuations in transverse velocity and magnetic fields and display a higher degree of correlation between the velocity and magnetic fluctuations (often described as a well-developed spectrum of quasi-incompressible *Alfvén waves* propagating away from the Sun). In the slow wind, this correlation occurs at a much lower level, while larger fluctuations in density and in the magnitude of the magnetic field are

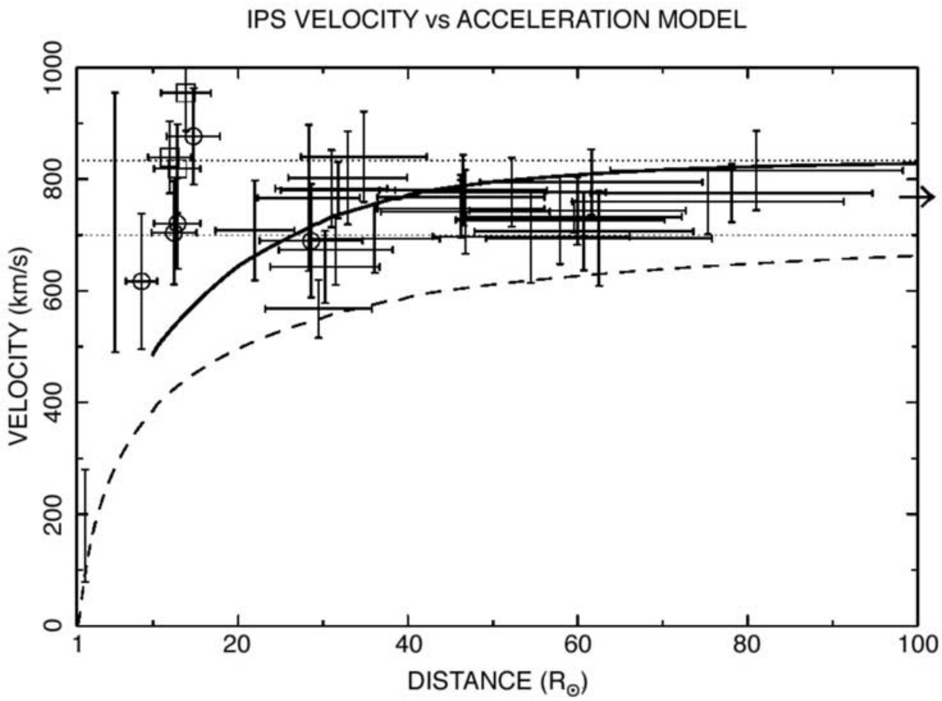

Figure 10. Apparent flow speed of the fast wind versus distance determined from radio scintillation measurements by European Incoherent Scatter (EISCAT), Very Long Baseline Array (VLBA), and Spartan 201-01, showing rapid acceleration of the solar wind at distances $\leq 10\ R_S$. These measurements rely on the phase shifts in radio signals caused by the movement of density structures across the line of sight and therefore contain the effects of compressive waves. Reprinted from *Grall et al.* [1996], by permission from Macmillan Publishers Ltd (*Nature*).

present, indicating a more evolved MHD turbulent state there. This difference in turbulence between fast and slow wind streams, together with the fact that slow wind distribution functions are much closer to equilibrium, suggests that the outward propagating wave flux contributes to the heating of the steady fast wind, while the slow wind heating is much more variable. It is not known, however, how the turbulent flux increases toward the Sun, whether it is sufficient to power coronal heating and solar wind acceleration, and how it is driven by time-dependent events in the photosphere, chromosphere, transition region, and lower corona.

[34] In situ measurements of plasma distribution functions, waves, turbulence, and electromagnetic fields from 0.3 AU to within a few R_S of the Sun, correlated with plasma and magnetic field structures, will make it possible to answer basic questions of coronal heating and solar wind acceleration: (1) How is the solar corona powered? (2) How is the energy channeled into the kinetics of particle distribution functions in the solar corona and wind? (3) How do such processes relate to the turbulence and wave-particle dynamics observed in the heliosphere?

3.1. Transfer of Energy to the Corona and Its Dissipation

[35] A large amount of kinetic energy is available in photospheric motions. The question is: How is this energy transmitted upward and dissipated, within a few solar radii of the surface, to heat the corona? The coincidence of magnetic and thermal structures suggests that the magnetic field plays a fundamental role in channeling, storing, and dissipating the energy, both via the emergence of photospheric flux tubes and through their continuous distortion and convection by the photospheric velocity fields. Photospheric motions on different timescales have different effects, which may be broadly divided into two categories: power at periods below a few minutes propagates in the form of MHD waves (AC) (see the recent review by *Ofman* [2005]), while power at lower frequencies is stored by currents in the coronal magnetic field (DC) (see *Narain and Ulmschneider* [1996, section 6] for a review of proposed DC heating mechanisms).

[36] Because of the high coronal temperatures, the resistivity of the coronal plasma is weak (i.e., magnetic Reynolds numbers are of order $S \sim 10^{12}$ based on collisional resistivity). Weak resistivity implies that the dissipation of MHD waves must occur via the development of steep gradients and small scales, through nonlinear steepening or a turbulent cascade, for example, or through phase mixing and resonant absorption. In the case of energy stored in DC currents, dissipation occurs by means of current sheet collapse and magnetic reconnection. Ultimately, both mechanisms require large electric fields, so that particle acceleration occurs, resulting in nonthermal particle distributions.

[37] Whether the solar corona is heated by low-frequency waves resulting from motions naturally arising in the

photosphere or whether the dominant energy source resides in the currents stored via slower field line motions has been the subject of strong debate. Among the MHD waves, only Alfvén waves would appear to survive the strong gradients in the chromosphere and transition region, because slow modes steepen into shocks while fast modes suffer total reflection. Transmitted waves propagate at large angles to the radial direction, since a 100 s wave with an Alfvén speed of 2000 km s^{-1} has a wavelength along the direction of the field of 2×10^5 km, while the perpendicular coherence will be at most 10^4 km. Longer-period waves must have an even larger anisotropy. Waves reaching the lower corona must therefore be shear Alfvén waves, although discrete coronal structures such as loops and plumes might channel surface waves and propagate energy as global oscillations as well.

[38] Several mechanisms for the dissipation of waves have been proposed, among which phase mixing [*Heyvaerts and Priest*, 1983] and resonant absorption [*Ionson*, 1978] are the most widely invoked. Both processes rely on gradients in coronal structures or, more generally, on the presence of nonuniform phase speeds, resulting in the corrugation of wavefronts and the development of small scales as the waves propagate. It is not clear, however, that wave dissipation by either process could occur within the distance required to produce the high-speed wind (i.e., 1.5 R_S from the coronal base in open field regions) [*Hansteen et al.*, 1997]. Phase mixing and resonant absorption might play a specific role in coronal structures such as plumes, where guided surface and slow mode waves have been remotely observed and modeled [*Ofman et al.*, 1999, 2000]. Alternatively, the upward transported waves may drive low-frequency turbulence and a quasi-perpendicular cascade involving counterpropagating waves [*Matthaeus et al.*, 1999] to provide the source for extended heating at smaller scales needed to drive the fast wind from coronal holes. In any of these scenarios, the details of the kinetic processes that convert small-scale fluid motions into thermodynamic internal energy remain to be discovered.

[39] *Parker* [1988] argued that most of the energy reaching the corona comes from the slow displacement of closed field lines in low-lying loops, which are tangled until they spontaneously develop current sheets and then reconnect, resulting in elementary dissipation events known as *nanoflares*. In this scenario, the energy for coronal heating is stored in presently unmeasured coronal magnetic field fluctuations. On the basis of coronal heating energy requirements, Parker estimated that 10^{24} ergs must be released per elementary event. MHD numerical experiments have shown how power law distributions in energy release are a natural outcome of the Parker scenario, with indices not far from those observed in X-ray flaring events [*Georgoulis et al.*, 1998]. The original nanoflare heating scenario has been strongly debated, observational work having focused mostly on the power law index characterizing the distribution of the panoply of small-scale energetic events observed in the corona, transition region, and network. Extrapolating the data to lower energies and inferring the total contribution of such events to coronal losses is subject to strong uncertainties [*Cargill and Klimchuk*, 2004]. However, measurement in the inner heliosphere of energetic particles and their spectra, as well as the measurement of the coronal magnetic field and its fluctuations at low heliolatitudes, where confined coronal plasma may be traversed, could provide important indirect evidence for the lower-energy scales to which bursty events extend.

[40] Recently, the role of low-lying loops and reconnection at transition region heights due to photospheric dragging of network and intranetwork fields (magnetic carpet versus canopy) has been stressed as a potential source of energy, in the form both of direct heat and of waves launched by reconnection [*Axford and McKenzie*, 1992; *Schrijver et al.*, 1997; *Longcope et al.*, 2003; *Fisk*, 2003]. High-frequency modes of this type (e.g., ion cyclotron waves) [*Marsch and Tu*, 2001] can propagate into the corona, where they can drive the heating of both protons and minor ions. Similar phenomena may be involved in the polar radial magnetic field inversions observed by the Ulysses spacecraft [*Yamauchi et al.*, 2004]. Reconnection, buffeting of field lines associated with photospheric oscillations, or direct field line dragging by photospheric velocity fields have also been invoked to account for the formation of chromospheric and coronal features such as spicules and macrospicules [*Sterling*, 2000], although no theory has yet been able to completely describe such phenomena.

[41] Comprehensive measurements of plasma and electromagnetic fluctuations in the inner solar wind ($<$20 R_S) are needed to determine how the energy that powers the corona and wind is dissipated and what the dominant dissipative structures are as well as the frequency spectrum of electromagnetic fluctuations. Small-scale magnetic reconnection occupies an important place in the closed field line Parker mechanism and in open field line cascades. Testing of these models requires local measurements of the signatures of small-scale reconnection, such as bidirectional plasma jets, accelerated particles, and magnetic field and velocity gradients along the trajectory.

[42] Energy transport and dissipation mechanisms strongly depend on the mean free path of particles in the coronal plasma, which varies drastically with distance from the Sun (from the base of the corona to the supersonic solar wind), as well as across coronal structures (coronal holes to helmet streamers). This dependence has led to the suggestion that coronal heating arises from energy stored in nonthermal wings of particle distribution functions generated between the chromosphere and transition region or, more generally, in the region where the solar atmospheric plasma changes from collisional to collisionless. The higher temperatures and subsequent outflows would then arise naturally through velocity filtration by the Sun's gravitational potential [*Scudder*, 1994]. To identify the coronal regions above which *Coulomb collisions* are negligible and to assess the contribution of the velocity filtration mechanism in shaping coronal distribution functions, measurement of electron and ion distribution functions out to large energies as a

function of distance from the Sun in the inner heliosphere is required.

3.2. Nonequilibrium Velocity Distributions in the Solar Wind

[43] The significant broadening of minor ion emission lines observed in coronal holes with Spartan and UVCS on SOHO results from unresolved ion motions and is indicative of high-temperature anisotropies in the coronal holes, with preferred heating in a direction perpendicular to the radial and preferential acceleration of minor ions over neutral hydrogen, which in the lower corona should be strongly coupled to protons [*Li et al.*, 1998; *Kohl et al.*, 1998]. Preferential heating of minor ions with respect to protons and temperature anisotropies are also observed in the fast solar wind, where in situ measurements have shown that the perpendicular temperature in the thermal core component of the proton velocity distribution is higher than the parallel temperature. In situ measurements have also shown that the magnetic moment is not conserved, implying that plasma turbulence heats the ions significantly in directions perpendicular to the magnetic field from 0.3 out to 1 AU and beyond. Whether this turbulent heating is the primary energy source closer to the Sun, however, is unclear; also, because the temperatures determined from remote sensing techniques are indirect and are dependent on empirical modeling, discriminating turbulent bulk perpendicular and parallel motions from real temperatures requires in situ measurement of proton, helium, and minor ion temperatures inside 0.3 AU. Such measurements would clarify the role of turbulence and wave-particle interactions in shaping the particle distribution functions and also provide a yardstick for remote sensing temperature observations. It must be emphasized that remote sensing measurements of the Lyman alpha line determine properties of the neutral hydrogen distribution, whose coupling to protons depends crucially on the density profiles; semiempirical models of the solar wind require an average mean proton temperature of at least 3 MK between 2 and 4 R_S, but only the direct measurement of proton temperatures in the corona (perhaps approaching or moving inside the temperature maximum radius at low latitudes) can lead to an understanding of the energetically dominant wave-particle interaction properties.

[44] In addition to the core component, the proton distribution in the fast solar wind has an accelerated beam component whose drift speed is comparable to the Alfvén speed, which is close to the alpha particle drift speed with respect to the protons [*Feldman et al.*, 1974; *Marsch et al.*, 1982; *Tu et al.*, 2004]. (The two principal explanations put forward for the presence of such beams are direct generation, in the jet superposition picture of solar wind formation, and wave-particle interactions in the solar wind acceleration region.) The relative drift of protons and alpha particles is observed beyond 0.3 AU in the solar wind and should reach enormous values if it remains close to the Alfvén speed approaching the Alfvénic point. Measurements of the shape of the proton and alpha particle distribution functions inside 0.3 AU can help determine how this drift originates, yielding clues about the responsible mechanisms.

[45] In situ measurements of the solar wind and remote sensing observations of coronal holes strongly implicate resonant interaction with ion cyclotron waves as the mechanism responsible for heating and accelerating coronal hole ions to generate the fast solar wind. The evidence pointing to this mechanism includes observations of extended proton heating, minor ion heating, equal thermal ion velocities, and greater-than-mass-proportional ion temperatures. A natural process that might lead to these effects is "cyclotron sweeping" [*Galinsky and Shevchenko*, 2000; *Hollweg and Isenberg*, 2002], which relies on the gradual decrease with distance from the Sun of the ion cyclotron frequency relative to the Alfvén wave frequency. Minor ions, with resonance at lower frequency, would therefore come into resonance closer in the corona, and naturally tap higher-energy regions of the turbulent spectrum, assuming a standard, decreasing shape for energy as a function of frequency. Although this process may work for minor ions, its efficiency is dramatically reduced for protons [*Ofman et al.*, 2002; *Isenberg*, 2004], calling its relevance into question as a whole. Near-Sun measurements of proton and alpha particle distribution functions and of high-frequency wave spectra, together with, wave mode analysis, are of key importance in determining the relevance of ion cyclotron waves in regulating solar wind acceleration processes.

[46] Other possibilities exist for converting collective plasma energy into thermal energy, thereby shaping plasma distribution functions: in addition to the cyclotron mechanisms discussed above, which feed on fluctuations that vary along the magnetic field, there are also a variety of processes that are powered by cross-field perpendicular fluctuations. Among these are *oblique wave* damping or *Landau damping*, weakly collisional and/or compressive damping, and mechanisms involving nonlinear dynamics of current sheets that might be formed by small-scale shears or reconnection activity. The last mentioned include kinetic (lower hybrid) plasma turbulence, electron solitary structures, mode conversion, and nonlinear beam instabilities. As an example, in the solar wind, there is evidence that the dissipation of kinetic Alfvén waves at large perpendicular wave numbers, due at least in part to Landau damping and gyroresonant effects, contributes significantly to plasma heating [*Leamon et al.*, 1998].

[47] To identify the heating mechanisms that operate in the corona and to assess their relative contributions to coronal heating, the near-Sun particles-and-fields environment must be sampled in situ. High- and low-frequency fluctuations responsible for wave-particle interactions and turbulence must be characterized, proton and alpha particle distribution functions and the temperatures of minor ion species and their anisotropies must be determined, and their relationship to fluctuations in the magnetic field and the bulk velocity field must be ascertained. These data will allow the basic interactions that shape the distribution functions in the solar wind acceleration region to be determined and will furnish the ground truth knowledge

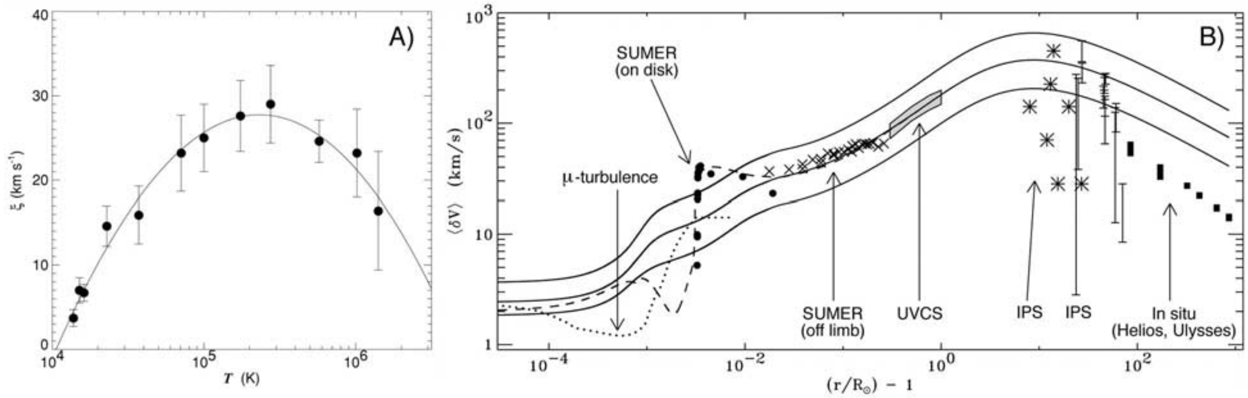

Figure 11. (a) Nonthermal component to line model broadening in the solar atmosphere as a function of temperature showing a maximum around 30 km s^{-1} at transition region heights [*Chae et al.*, 2002]. (b) Composite of observations of magnetic field and velocity field fluctuation amplitude with height in the solar atmosphere [*Cranmer and van Ballegooijen*, 2005]. Note the gap between the data labeled UVCS and interplanetary scintillation (IPS), where in situ measurements of velocity and magnetic field fluctuations are needed to clarify the role of such fluctuations in coronal heating and solar wind acceleration. Both images are reproduced by permission of the AAS.

needed to answer the most basic questions about energy dissipation and heating in the corona.

3.3. Corona's Imprint on the Solar Wind

[48] The fast wind displays Alfvénic turbulence, i.e., fluctuations sharing many properties of large-amplitude Alfvén waves propagating away from the Sun (including nearly vanishing magnetic pressure fluctuations) but with a flat frequency (f) spectrum, $E_f \sim 1/f$. The origin of the shape of this "flicker noise" spectrum is not understood, although it is suggestive of the presence of scale-invariant processes, such as reconnection, in the lower corona [*Matthaeus and Goldstein*, 1986]. At higher frequencies the spectrum gradually steepens, which is presumably associated with an active turbulent cascade. The breakpoint between the two spectral forms is, roughly, at the measured correlation scale of the fluctuations, which gradually evolves toward lower frequency with increasing heliocentric distance.

[49] Is the lower-frequency $1/f$ spectrum a remnant of the wave flux that contributes to plasma heating in the lower corona? The existence of a broad spectrum is evidence in itself of significant dynamic evolution; otherwise, significant traces of transmission through the coronal cavity should be found, in the form of preferred frequencies or broad "lines" in the spectrum [*Velli*, 1993]. However, if the very low frequency solar wind fluctuations are remnants of coronal heating, then in situ observations near the Sun should reveal additional required factors, such as a flux of "inward"-type Alfvénic fluctuations, a possible component of compressive fluctuations, and signatures of an incompletely understood mechanism for containing the inward waves in the presence of the turbulence near the Alfvénic critical point. There has been some debate as to whether signatures of the global solar oscillations, such as the 5-min photospheric p modes, survive in the solar wind, as measurements are very close to the noise level as measured in situ [*Thomson et al.*, 1995]. Near-Sun measurements can determine whether such oscillations are present in the corona before there is time for nonlinear dynamics to smooth them out.

[50] Simple extrapolation, along with interplanetary scintillation observations [*Canals et al.*, 2002], suggests that root-mean-square (RMS) velocity field fluctuations of about 200 km s^{-1} at the Alfvénic critical point should be observable in the inner heliosphere, while at the base of the corona, limits obtained from spectral line widths indicate a turbulent velocity near the transition region of 30 km s^{-1} [*Chae et al.*, 1998, 2002] (Figure 11a). Observations of fluctuation amplitudes from the Sun out to 1 AU are summarized in Figure 11b [*Cranmer and van Ballegooijen*, 2005]. Such measurements appear to be broadly consistent with an Alfvén wave propagation that is modified very little by nonlinear effects, in which case, there would be little or no contribution from these waves to coronal heating. Particles-and-fields measurements within a few R_S of the Sun should unequivocally determine whether the currently observed fluctuations are, in fact, one of the principal agents in the coronal heating and wind acceleration process.

[51] How is the Alfvénic turbulence observed in high-speed solar wind streams generated and how does it evolve? How much energy is available, and how is it distributed in space and time? What wave modes and/or structures are excited? The answers to these questions, which are critical for understanding coronal heating and solar wind acceleration, require measurements of the fluctuations of velocity, density, temperature, and magnetic fields from 0.3 AU down to 4 R_S. Such measurements would also make it possible to ascertain whether the observed in situ fluctuations are indeed the remnant of the coronal heating process and how their evolution is coupled to the evolution of the thermodynamic properties of the plasma itself, principally temperature, density, velocity, and average magnetic field.

[52] Apart from determining the initial conditions for the origin of the solar wind turbulent spectra, coronal processes

have a large impact on other solar wind properties. For example, the composition of the solar wind and its variation with wind speed, which also follows a bimodal pattern, show that the slow wind is enhanced in low first ionization potential (FIP) elements with respect to photospheric values [*Zurbuchen et al.*, 2002]. This enhancement most probably results from the longer confinement time, in or around closed coronal loop-type structures, of the slow solar wind plasma. To fully exploit the information provided by FIP measurements about the coronal processes associated with the production of the slow and fast winds, it would be desirable to measure the abundances of heavy ions in the slow and fast wind close to the Sun, ions that to date have been observed only remotely or far from the Sun in situ. In addition, measurements near the Sun may reveal the presence of light FIP elements, such as Na, which, due to their low abundance, have not been observed so far. The measurement of the FIP effects in these elements can provide strong constraints on the mechanism responsible for the FIP effect and yield clues to the ionization processes in slow and fast solar wind plasma.

[53] The outer solar corona between 5 and 20 R_S plays a fundamental role in determining large-scale properties such as solar wind angular momentum loss and global heliospheric structure. This is because the Alfvénic critical surface, where the solar wind speed overtakes the Alfvén speed, defines the point where the plasma ceases to corotate with the Sun, i.e., where the magnetic field loses its rigidity to the plasma. This is also the region where the velocity gradients between the fast and slow speed streams develop, determining the initial conditions for the development, further out, of *corotating interaction* region*s* (CIRs). Precise measurements of the plasma flow, magnetic field, and their gradients over this critical distance range would make it possible to determine the initial conditions for the development of heliospheric structure, enabling a predictive approach to mean global heliospheric structure based on actual coronal measurements.

4. ENERGETIC PARTICLE ACCELERATION AND TRANSPORT

[54] The current paradigm [e.g., *Reames*, 1999] defines two classes of solar energetic particle (SEP) events. In gradual events, SEPs are accelerated by CME-driven shocks and are characterized by roughly coronal abundances and charge states. Impulsive events are generally much smaller events associated with impulsive X-ray flares and are characterized by enrichments in ^{3}He, electrons and heavy ions such as Fe, with charge states characteristic of temperatures ranging from ~5 to 10 MK. This paradigm distinguishes between two separate acceleration processes and acceleration sites, both driven by eruptive events on the Sun: (1) CME-driven shock acceleration starting in the high corona and continuing into interplanetary space and (2) acceleration at the flare site, presumably driven by magnetic reconnection. Both processes are known to operate in larger SEP events, and studies at 1 AU during solar cycle 23 present a complex picture of events that often exhibit characteristics of both gradual and impulsive SEP events [e.g., *Cohen et al.*, 1999; *Cane et al.*, 2003; *Tylka et al.*, 2005]. In addition to such transient energetic events, observations at 1 AU show a continual outflow of intermediate-energy particles from the Sun extending from suprathermal energies to >10 MeV nucleon^{-1}. The mechanisms responsible for the acceleration of these particles are not known.

[55] Distinguishing the various acceleration processes occurring at the Sun on the basis of data acquired at 1 AU is problematic. Transport through the interplanetary medium washes out the time structure, reduces the intensities by orders of magnitude, and leads to mixing of particles from different acceleration sites. In situ measurements made within a few R_S would not suffer from transport effects because the energetic particles would be sampled close to their acceleration sites on the Sun and will explore, in situ, acceleration sites in the corona and inner heliosphere. In particular, recent results from ACE, SOHO, and Wind point to the increasing importance of the high corona (2 R_S < r < 20 R_S) as an acceleration site for energetic ions and electrons, a region that, if sampled directly, would provide answers to key questions important for understanding solar energetic particle acceleration and transport.

4.1. Role of Shocks, Reconnection, Waves, and Turbulence

[56] In ^{3}He-rich SEP events, abundance ratios of ^{3}He/^{4}He commonly exceed that in the solar wind (~5 × 10^{-4}) by 3 orders of magnitude or more. In addition, heavy nuclei abundances (relative to coronal values) tend to increase with increasing mass, resulting in roughly tenfold enhancements of Fe/O and in enhancements of "ultraheavy" (Z > 30) elements by factors as large as 10^2 to 10^3 [*Mason et al.*, 2004; *Reames and Ng*, 2004] (see Figure 12). Explanations of this highly selective fractionation have generally focused on plasma processes that heat and/or accelerate ions in a certain range of charge/mass ratio, including models based on electromagnetic ion cyclotron waves (see, e.g., the review by *Miller* [1998]). However, *Mason et al.* [2004] have suggested that these processes fail to account for the overall composition pattern and suggested that coronal shocks may be the accelerating agent in impulsive SEP events.

[57] About 1000 impulsive SEP events per year are estimated to occur on the Sun during solar maximum, but the number may be much larger because many small events undoubtedly go undetected at 1 AU. Figure 13 shows a series of ~10 events observed at 1 AU during a several day period. Observations of the same ^{3}He-rich SEP event by IMP 8 at 1 AU and by Helios at 0.32 AU show that the event is ~100 times more intense at 0.32 AU and much more localized in time (Figure 14). Observed even closer to the Sun, these events will appear as intense bursts of only minutes in duration. In situ energetic ion measurements, together with simultaneous solar observations from 1 AU, should make it possible to trace such events to the flare site,

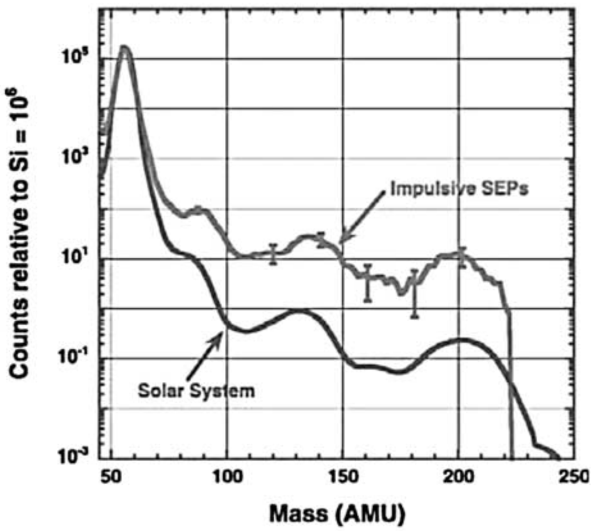

Figure 12. Nuclei with mass >90 ($Z > 40$) are overabundant in impulsive SEP events (compared to solar material) by factors ranging from ∼10 to ∼50 when normalized to Fe. Since Fe is itself overabundant by a factor of ∼10, the $Z > 40$ overabundance is even greater when normalized to He or oxygen (observations by *Mason et al.* [2004]). The origin of these over abundances is not understood. Reproduced by permission of the AAS.

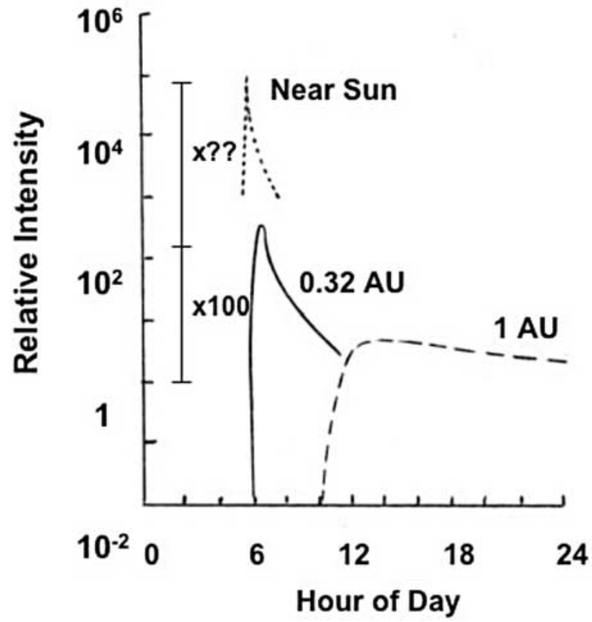

Figure 14. Time profiles of an impulsive ^{3}He-rich event observed at 1 AU on 17 May 1979 by ISEE-3 and at 0.32 AU by Helios-1 (based on data of *Mason et al.* [1989]). Both spacecraft were magnetically well connected to the flare site. Note that the peak intensity is ∼100 times greater at 0.32 AU. Closer to the Sun the event will be even more localized in time.

to measure the flare properties, and to obtain the underlying magnetic field configuration. In addition to composition measurements, measurements of near-relativistic ($V > 0.1$ c) electrons from these events within a fraction of a minute of their release would be particularly important for untangling acceleration processes because the electron acceleration sites can be sensed remotely by microwave radio emission or hard X rays. As is the case with the energetic ion measurements, in situ observations of gamma rays and neutrons from these solar flare events would provide information on the accelerated particle components on closed field lines in the solar atmosphere.

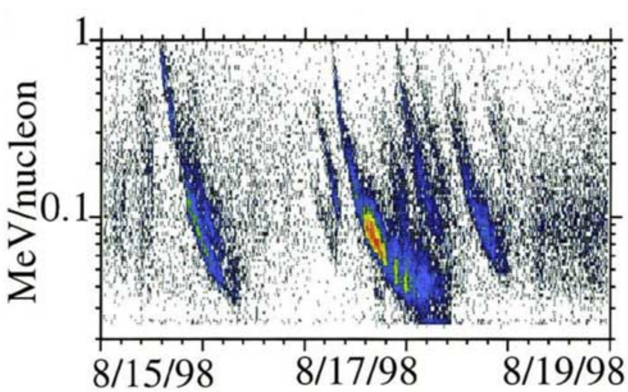

Figure 13. Energy versus time plot showing a series of impulsive events observed by ACE in 1998 [*Mason et al.*, 1999]. Because of velocity dispersion, the highest-energy particles arrive first. Reproduced by permission of the AAS.

[58] Although the occurrence rate of SEP events is greatly reduced at solar minimum, strong evidence suggests that particle acceleration occurs continuously on the Sun or in the inner heliosphere, even at solar minimum. All solar wind species that have been measured (H^+, He^+, and He^{++}) exhibit *suprathermal tails* that extend up from several times the solar wind speed (∼10 keV nucleon^{-1} (Figure 15). These tails are more prominent in the ecliptic than over the poles, and they are continuously present, even in the absence of solar activity or interplanetary shocks [e.g., *Gloeckler et al.*, 2000]. The fact that even interstellar pickup He^+ exhibits a suprathermal tail suggests that the acceleration occurs (by some unknown process) in the inner heliosphere [e.g., *Le Roux et al.*, 2002]. However, evidence also indicates that ^{3}He is continuously accelerated at the Sun, even during the quietest periods, suggesting that more or less continuous acceleration may be occurring in microflares such as those observed by the Reuven Ramaty High Energy Solar Spectroscopic Imager (RHESSI) [*Krucker et al.*, 2002]. The small-scale, randomly occurring "component" reconnection that typifies microflares may be an indicator of a scale-invariant dissipation process that not only heats coronal plasma but also produces a stochastic component of the electric field that contributes to particle acceleration. The production of these dissipative structures may be related to the small-scale termination of the cascade of plasma turbu-

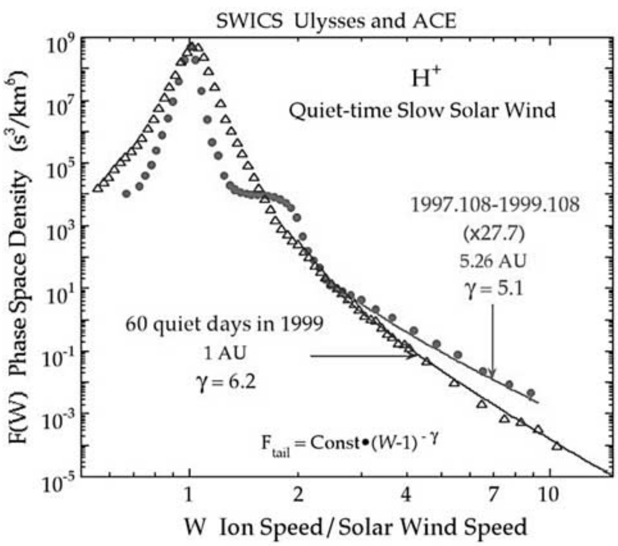

Figure 15. All solar wind species somehow develop suprathermal tails extending to >100 keV nucleon^{-1} somewhere between the Sun and 1 AU, as illustrated in these data from Ulysses and ACE. The mechanism for creating these tails is not known. Note that 10 times the solar wind speed is close to ~100 keV nucleon^{-1}.

lence that connects large with small scales and may be distributed throughout the heliosphere [*Matthaeus and Lamkin*, 1986; *Ambrosiano et al.*, 1988].

[59] Investigation of the role of microflares and other processes in the continuous acceleration of energetic particles at the Sun requires measurements of the plasma, fields, and energetic particles in the inner heliosphere at distances where the particle intensities will be orders of magnitude larger than at 1 AU. Hard X-ray, gamma ray, and neutron observations can also reveal the occurrence of continuous particle acceleration on the Sun. Solar neutron observations in the near-Sun environment are of special interest because low-energy neutrons that do not survive to 1 AU can only be observed close to the Sun. Approximately 1 MeV (10 MeV) neutron intensities at 5 R_S are $\sim 1.5 \times 10^{10}$ (3.7×10^6) times greater than at 1 AU. Neutron observations close to the Sun may reveal evidence of small nanoflares, which have been suggested as a principal source of energy for heating the corona, as well as contributions to the continuous background of intermediate-energy seed protons through neutron beta decay.

4.2. SEP Production: Necessary Conditions

[60] SOHO has observed more than 8000 CMEs since 1996 but has measured only about 100 large SEP events during this same time period (particle intensities >100 (cm^2 sr)$^{-1}$ > 10 MeV). The acceleration mechanism (first-order Fermi acceleration) in gradual SEP events is generally well understood. Moreover, it is known that faster CMEs can form shocks more easily and that shocks driven by fast, wide CMEs accelerate particles more efficiently. It remains a mystery, however, why, for a given CME speed, the peak intensity of >10 MeV protons can vary by a factor of $\sim 10^4$ [*Kahler*, 2001].

[61] To forecast large SEP events reliably, it is necessary to determine why some CMEs accelerate particles more efficiently than others. The suggested possibilities include (1) the presence or absence of a preexisting population of suprathermal ions, left over either from a previous gradual event [e.g., *Kahler*, 2001] or from small impulsive flares [*Mason et al.*, 1999]; (2) the presence or absence of successive, interacting CMEs [*Gopalswamy et al.*, 2002]; (3) preconditioning and production of seed particles by a previous CME [*Kahler*, 2001; *Gopalswamy et al.*, 2004]; (4) improved injection efficiency and acceleration rate at quasi-perpendicular (as opposed to quasi-parallel) shocks [*Tylka et al.*, 2005]; (5) variable contributions from flare and shock-accelerated particles [*Cane et al.*, 2003], including acceleration of associated flare particles by the shock [*Li and Zank*, 2005; *Cliver et al.*, 2004]; and (6) production of SEPs in polar plumes, where shock formation may be easier [*Kahler and Reames*, 2003].

[62] Timing studies have shown that in gradual events SEPs are first accelerated at distances between ~3 and 12 R_S [*Kahler*, 1994; *Mewaldt et al.*, 2003]. Formation of the CME-driven shock requires that $v_{\rm cme} > v_{\rm sw} + v_{\rm fast}$, where $v_{\rm fast} \approx (v_{\rm A}^2 + c_{\rm s}^2)^{1/2}$, $v_{\rm A}$ is the Alfvén speed and $c_{\rm s}$ is the sound speed [see, e.g., *Kahler and Reames*, 2003]. It has therefore been suggested that SEPs originate beyond ~3 R_S because there is a peak in the Alfvén velocity at ~3 R_S, such that it is only beyond this radius that shocks can be easily formed and sustained for typical CME speeds [e.g., *Gopalswamy et al.*, 2001] (Figure 16). In MHD simulations of SEP events driven by coronal shocks [e.g., *Zank et al.*, 2000; *Sokolov et al.*, 2004] it is necessary to assume or model a variety of conditions in the region where gradual SEP events originate, including the magnetic field and density profiles, the solar wind and Alfvén speeds, the density of seed particles, and turbulence levels that determine the particle diffusion coefficient. Direct measurements of the solar wind and magnetic field close to the Sun, of the density and energy spectrum of suprathermal seed particles, and of the spectrum of magnetic turbulence are of critical importance in providing needed constraints for understanding SEP events.

[63] During solar maximum conditions there is about an 80% probability (J. Feynman et al., Near-Sun energetic particle environment of Solar Probe: Phase 1, unpublished report, October 2000) that a spacecraft passing through the inner heliosphere would encounter particle intensity levels characteristic of large SEP events at 1 AU (e.g., >100 particles (cm^2 sr s)$^{-1}$ with E >10 MeV) and only a ~10–20% probability of collecting data while a CME-driven shock is accelerating >10 MeV particles inside 100 R_S. Nonetheless, measurements of the ambient conditions that exist prior to such events would be of enormous value to our efforts to understand SEP acceleration and transport. In addition to such large episodic events, there is a significant level of ongoing particle acceleration that can only be observed near the Sun because the intensity of

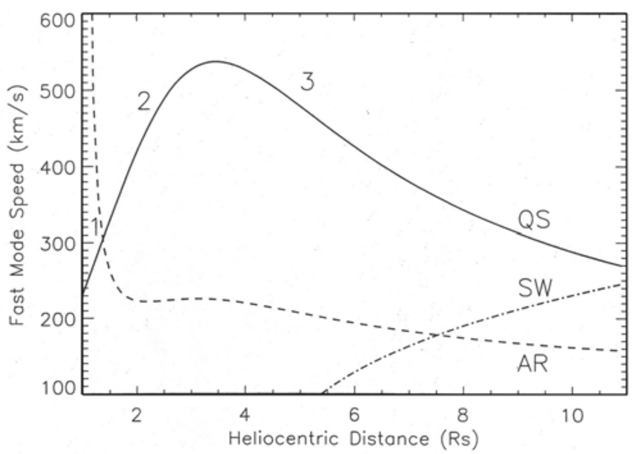

Figure 16. Estimated speed profile of the fast magnetosonic mode (Vfast) in the quiet Sun (QS) and in the active region (AR) coronas [from *Gopalswamy et al.*, 2001]. Conditions for shock formation differ in the three regions marked 1, 2, and 3. A CME can form a shock if the CME speed exceeds the sum of Vfast plus the solar wind speed (SW), one estimate for which is shown above. Shocks formed inside ~3 R_S will not propagate into the quiet corona beyond ~3 R_S unless they have speeds greater than ~540 km s^{-1}; however, the CME driver could form a new shock once beyond the peak. The height of the peak in the Vfast curve depends on the actual density and magnetic field values in a given location, but the shape of the curve will be the same. Measurement of these quantities and their variability near the Sun would reveal where and how easily shocks can form and would provide ground truth for models of SEP acceleration by fast CMEs.

these background events is too small to be detected at 1 AU but would be orders of magnitude greater in the near-Sun region. Capturing a large SEP event would yield fascinating data, but measurements of even the expected low-level activity would provide definitive information on the unknown details of near-Sun SEP acceleration and transport.

4.3. SEP Transport

[64] Ulysses measurements have shown that solar energetic particles (SEPs) can reach high latitudes [*McKibben et al.*, 2001]. Three explanations for these observations have been proposed: (1) the CME shocks accelerating the particles extended to high latitudes and crossed the interplanetary magnetic field lines connecting to Ulysses; (2) significant particle cross-field diffusion took place; and (3) magnetic field lines connecting high latitudes with low-latitude active regions existed in the solar corona, allowing particles to reach high latitudes close to the Sun. On the basis of a comparison of onset times at Ulysses with onset times in the ecliptic for events with the same solar origin, *Dalla et al.* [2002] conclude that high-latitude events are not compatible with direct scatter-free propagation along a magnetic field line but rather that the large path lengths and late release times suggest that propagation to high latitudes requires scattering. Energetic particle measurements are needed at all heliolatitudes to determine how scattering properties from the corona into the solar wind vary with magnetic field and turbulence intensities. These measurements, together with magnetic field measurements, would also help to identify large-scale deviations from the Parker spiral configuration and to determine their role in energetic particle scattering.

[65] Energetic electrons are observed in both impulsive and gradual SEP events. Because of the electrons' near-relativistic velocities, the onset times of electron events at 1 AU are often used to deduce SEP release times near the Sun for comparison with their associated electromagnetic signatures. Surprisingly, the deduced release times almost always appear to be delayed by ~10 min with respect to electromagnetic signatures such as soft X-ray and optical emissions from flares and associated radio emissions [e.g., *Krucker and Lin*, 2000; *Haggerty and Roelof*, 2002]. This discrepancy has resulted in considerable debate concerning its cause, whether storage and subsequent release of the electrons, longitudinal propagation of the acceleration mechanism from the flare site to the injection site, or radial transport of the acceleration mechanism in the form of a CME-driven shock [*Haggerty and Roelof*, 2002]. Close to the Sun, propagation delays will be minimized, and energetic electron measurements combined with interplanetary magnetic field observations can reveal where and how particles are released from the Sun and/or accelerated in interplanetary space.

5. NEAR-SOLAR DUST

[66] In addition to providing data needed to answer the questions of coronal heating and solar wind acceleration, measurements of the near-Sun particles-and-fields environment can supply useful information about the circumsolar cloud of cosmic dust. The origin of dust in the inner solar system is not well understood. Its ultimate source is thought to be the release of dust from comets and asteroids and the breakup of meteoroids (Figure 17). Subsequent dust-dust collisions lower the average mass of the dust particles. Dust orbital motion combines with Poynting-Robertson deceleration to increase the dust number densities toward the Sun [*Burns et al.*, 1979]. Inward from 1 AU, the fragmentation of cometary meteoroids locally is believed to produce a majority of dust particles [*Grün et al.*, 1985; *Ishimoto*, 2000; *Mann et al.*, 2004]. Dust particles attain electric surface charge through photoionization, electron emission, and interaction with the solar wind. While larger (>1 μm) particles move primarily in Keplerian orbits, smaller charged grains are deflected by the interplanetary magnetic field. The degree of deflection depends on the surface charge, which has not yet been directly measured for dust particles in space, and on the magnetic field magnitude and direction and their variation in time [*Mann et al.*, 2000]. Nanometer-sized dust particles can be picked up by the solar wind and accelerated up to solar wind velocity. In addition, dust dynamics is likely to

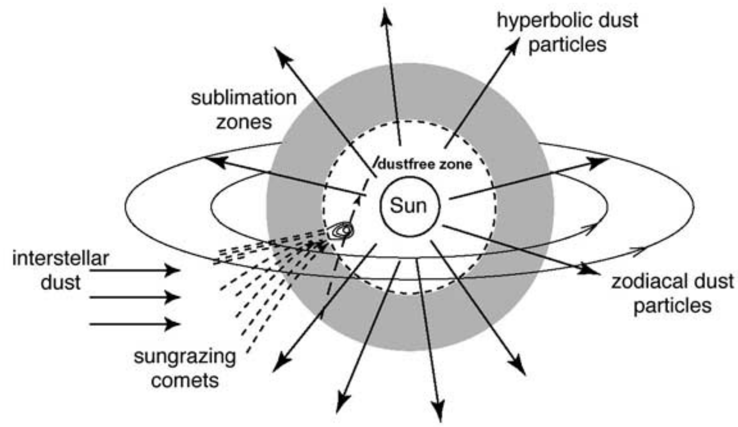

Figure 17. Sketch illustrating the dust environment near the Sun. Most of the dust near the Sun is bound in Keplerian, roughly circular orbits near the ecliptic, although some dust particles are ejected by radiation pressure on hyperbolic trajectories as β meteoroids. Comets and asteroids are the principal sources of the solar dust cloud, with smaller contributions from Sun-grazing comets and interstellar dust. Reprinted from *Mann et al.* [2004, Figure 14] with kind permission of Springer Science and Business Media. Copyright 2004 Kluwer Academic Publishers.

be influenced by such events as coronal mass ejections, which may even lead to dust destruction [*Misconi*, 1993; *Ragot and Kahler*, 2003].

[67] The interaction of dust in the inner heliosphere with the solar wind plasma influences not only the dust population but also the local plasma and gas environment. Notably, dust grains in the inner heliosphere are important as a source of *pickup ions* and protons as well as heavier species, which differ from the solar wind in their charge state and velocity distribution. These "inner source" pickup ions are potential candidates for subsequent acceleration and may contribute to the anomalous cosmic ray population [*Cummings et al.*, 2002]. Collisional evaporation, particularly in cometary meteoroid trails, is expected to influence the solar wind parameters measured locally. For example, a recent study shows that dust collisions in the inner solar system can produce some of the heavy species in amounts comparable to the observed inner source fluxes [*Mann and Czechowski*, 2005]. The material released in such collisions may be responsible for the enhancements of the interplanetary field measured by Ulysses in association with meteoroid trails (Figure 18) [*Jones et al.*, 2003]. These enhancements (which last for minutes to hours, are clustered in space, and occur more frequently in the inner solar system) may be the result of mass loading of the solar wind plasma induced by collisional vaporization in the dust trails [*Mann and Czechowski*, 2005]. It is still an open question how noble gases observed in the inner source are produced, with the solar wind/surface interactions being a distinct possibility. Ion composition measurements of inner source pickup ions in the near-Sun environment would provide information both about the composition of the circumsolar dust and about its spatial distribution. Particles-and-fields measurements, together with dust impact measurements, would reduce the uncertainties in our knowledge and models of dust in the inner heliosphere. In situ dust measurements near

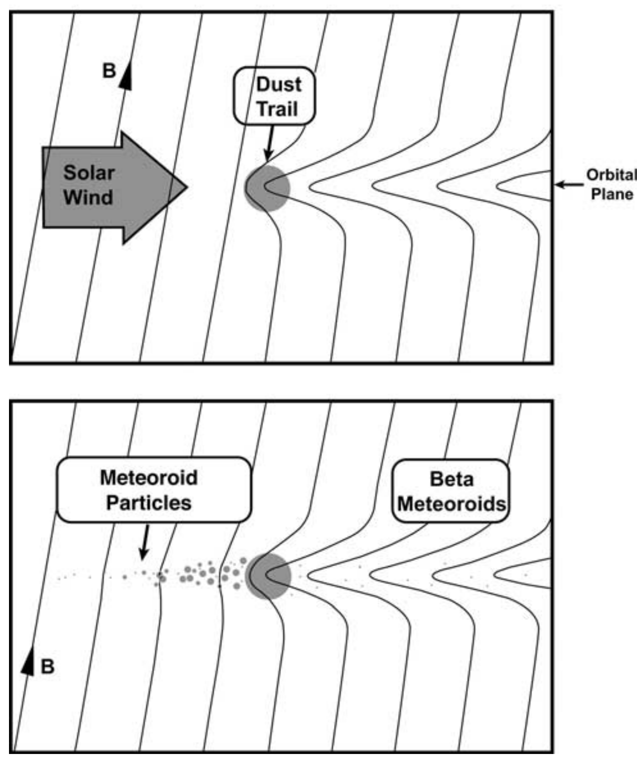

Figure 18. Cross-sectional sketch of cometary dust trail illustrating the formation of an interplanetary field enhancement (IFE). Such IFEs have been observed with Ulysses and correlated with meteoroid trails. It is hypothesized that the IFEs result from mass loading of the solar wind by material produced by collisional vaporization in dust trails. Reprinted from *Jones et al.* [2003], with permission of Elsevier.

the Sun would, moreover, have a direct bearing on certain astrophysical problems, with the circumsolar dust cloud serving as an analogue for circumstellar dust clouds, for example.

6. CONCLUSION

[68] Nearly half a century has passed since the publication of E. N. Parker's theory of the solar wind [*Parker*, 1958]. The properties and structure of the solar wind, including its component of heavy ions, have been extensively measured at high heliolatitudes as well as in the ecliptic and at distances far beyond the orbit of Pluto. The corona and transition region have been imaged with unprecedented high resolution, revealing a complex architecture of loops and arcades, while photospheric magnetography has uncovered the "magnetic carpet" of fine-scale flux bundles that underlies the corona. Observational advances have been accompanied by advances in theory and modeling, with both kinetic and MHD models offering plausible scenarios to explain coronal heating and solar wind acceleration. We now know more about the corona and the solar wind than ever before. Yet the two fundamental questions, raised by the spectroscopic studies of Bernard Lyot and others in the 1930s and 1940s and by the confirmation of Parker's theory early in the space age, remain unanswered: Why is the Sun's corona several hundred times hotter than the photosphere? How is the solar wind accelerated?

[69] The answers to these questions can be obtained only through in situ measurements of the solar wind as close to the Sun as possible. To date, however, the closest any spacecraft (Helios 1 and 2) has come to the Sun is 0.3 AU (65 R_S), which lies far outside the region where the acceleration of the solar wind occurs. Thus the need remains for a probe that will venture inside 0.3 AU, into the unexplored inner reaches of the heliosphere where the solar wind is born, and make in situ measurements of the solar wind plasma, energetic particles, and electromagnetic fields as close to the Sun as possible. Such a mission, which must survive in the extreme environment near the Sun, presents significant technical challenges. However, the recently concluded mission implementation and engineering study conducted under the direction of the Solar Probe STDT has demonstrated that a Solar Probe mission is technically feasible and can be accomplished within reasonable resources. The National Research Council's "decadal survey" in solar and space physics recommended implementation of a Solar Probe mission "as soon as possible" [*National Research Council*, 2003, p. 56], while NASA's Sun-Solar System Connection Roadmap identifies Solar Probe as a "flagship" mission that "is ready to fly and is our highest priority for new resources" [*NASA*, 2005b, p.12]. We thus have good reason to hope that Solar Probe, first proposed in October 1958, the month in which NASA was founded, will at last become a reality. Solar Probe will not only resolve fundamental questions about the heating of the corona and the acceleration of the solar wind, questions whose answers have so far eluded us. However, as noted by the STDT, it will give rise to new ones with which future generations of scientists must grapple [*NASA*, 2005a, p. ES-4]: "And as with any great voyage into uncharted realms, Solar Probe's journey to the Sun holds the promise of many more unanticipated discoveries—new mysteries to challenge humankind's ever-expanding knowledge of our home in the universe."

GLOSSARY

Active region: Arch-like magnetic field structure in the solar corona with a temperature of a few million degrees. Active regions bridge the opposite magnetic polarities in sunspots, where the magnetic flux is highly concentrated. Flares, characterized by sudden, intense, collimated releases of energy, often occur within active regions.

Alfvén speed: The characteristic speed of small-amplitude Alfvén waves in a magnetized plasma.

Alfvén wave: An oscillation in magnetic field lines that carry plasma at a frequency much below the ion cyclotron frequency. The wave travels at the Alfvén speed in the direction of the background magnetic field.

Chromosphere: A layer of cool gas in the solar atmosphere that separates the cooler photosphere from the hot corona above. With a temperature of about 20,000 K, it is characteristic of the red emission seen around the Sun during total solar eclipses.

Corona: The outermost, most tenuous region of the solar atmosphere. Characterized by temperatures as high as a few million degrees, it extends out into interplanetary space, producing the solar wind.

Coronal bright points: Miniature active regions, also known as X-ray bright points. They tend to overlie regions of positive and negative magnetic polarity and flash on and off with lifetimes of minutes to hours. Temperatures of these bright points can exceed 1,000,000 K.

Coronal hole: A region that appears darker than the rest of the corona when observed in ultraviolet or X rays. The average magnetic field in a coronal hole has a dominant polarity, despite the preponderance of opposite polarity bipoles scattered across its surface. Coronal holes dominate the polar caps of the Sun during the low-activity period in its cycle. They are often associated with the flow of fast solar wind, with speeds exceeding 600 km s^{-1} in interplanetary space.

Coronal mass ejection: A transient event frequently in the form of a large bubble of plasma expanding outward from the Sun. Such events are typically observed in white light with a coronagraph blocking the intense radiation from the solar disk. The ejection involves large quantities of mass (10^{15}–10^{16}g) and magnetic flux from the solar corona into interplanetary space. These events are often associated with solar flares and the eruption of prominences. They also produce the largest geomagnetic storms observed at Earth.

Coronal streamer, helmet streamer, streamer stalk: Long-lived structures, around 3–10 times denser than the surrounding regions, which extend from the base of the corona into interplanetary space. Generally localized around the equator at solar minimum, streamers appear to fill the corona in an almost spherically symmetric manner at solar maximum. Starting with a wide base at the Sun, they taper with distance toward an axis, also referred to as stalk, giving them a helmet-like appearance. The latter has been identified with a current sheet separating regions of opposite magnetic polarity and the locus of the slowest solar wind. The bulge at the base of a streamer, a consequence of saturation in white light images, is often attributed to closed magnetic structures.

Corotating interaction region: A region in interplanetary space where fast solar wind streams overtake slower streams, producing shock waves and intense magnetic fields. These regions tend to corotate with the Sun and are most prominent during solar minimum.

Coulomb collisions: Collisions between charged particles due to the Coulomb force acting between them. Such collisions normally result in momentum and energy transfer between particles.

Current sheet: A thin layer separating large-scale regions of different magnetic polarities in a plasma. Consistent with Ampère's law, high current density is observed in such layers.

Filling factor: The ratio between the volume or surface (e.g., a coronal loop or its photospheric foot point) apparently "filled" by a physical quantity (e.g., plasma density, magnetic flux) and the volume or surface actually occupied. The difference between the apparent and actual filled volume or surface may be the result of measurement effects. The term is often also used to mean the ratio between the volume or surface occupied by a physical quantity and the total volume of interest.

First ionization potential: The energy, generally measured in electron volts (eV), required to strip a neutral atom or molecule of a single electron.

Flare: An event associated with the rapid release of large quantities of energy (10^{32}–10^{33} ergs in 10^2–10^3 s) from a highly localized region in the solar corona.

H alpha surge: Collimated jet of chromospheric gas seen as a dark feature in H alpha images. These jets move at speeds of 20–200 km s^{-1} and have a lifetime of 10–20 min. Like X-ray jets, these surges are thought to be produced by reconnection between emerging and existing magnetic flux regions.

Ion cyclotron wave: A low-frequency electrostatic ion wave which propagates nearly perpendicular to the magnetic field ($\mathbf{k} \perp \mathbf{B}$).

Landau damping: A characteristic of collisionless plasmas where magnetohydrodynamic waves are damped and release their energy to the ambient plasma, without energy dissipation by collisions. Also known as resonant damping.

Magnetic carpet: A recently coined term referring to ultraviolet emission from small-scale mixed polarity magnetic fields scattered throughout the corona. The energy dissipated through the emergence, cancellation, coalescence, and fragmentation of these magnetic fields is thought to be a key process in heating the corona.

Magnetic network: A somewhat regular honeycomb like pattern covering the solar surface, produced by supergranular convection cells with magnetic fields concentrated at their boundaries. This regular pattern is disrupted only in sunspots.

Nanoflare: Very small flare with an energy content many decades less than that of the largest flares, observed to occur throughout the solar surface. Nanoflares have been proposed as a source of coronal heating.

Oblique wave: A wave propagating neither parallel nor perpendicular to a background magnetic field.

Parker spiral: The Archimedean spiral structure of the interplanetary extension of the Sun's magnetic field. This spiral structure is due to the Sun's rotation and to the fact that magnetic field lines are embedded or "frozen in" to the outflowing solar wind plasma.

Photosphere: The lowest and coolest layer of the Sun's atmosphere, which is observed as the Sun's visible "surface." It is about 500 km thick and has a density of approximately 10^{23} particles m^{-3}.

Pickup ion: Singly charged ions detected in the solar wind whose primary sources are (1) neutral atoms from the interstellar medium and (2) an inner source produced by solar wind interactions with dust grains near the Sun. Pickup ions are the seed population for anomalous cosmic rays and are used as a diagnostic tool to determine the density of matter in the interstellar medium.

Polar plumes: Magnetically open structures, denser than their surroundings, which appear to originate from the polar regions of the Sun.

Pressure-balanced structure: A plasma structure maintained by a balance between thermal and magnetic pressures.

Reconnection: The merging of magnetic flux tubes of opposite polarity to create a new magnetic topology, releasing energy in the process.

Solar wind: A fully ionized and magnetized plasma, composed primarily of protons and electrons, along with a few percent of alpha particles (He^{++}) and traces of other highly ionized species, streaming continuously outward from the Sun.

Spicule and macrospicule: A spicule is a short-lived, narrow jet of gas, less than 10,000 km in length, always visible in H alpha in the chromosphere, primarily at the edges of supergranular cells. A macrospicule is a giant spicule, roughly 10 times larger, and observed much less frequently.

Suprathermal tail: The high-velocity tail observed in a phase space distribution function where particles deviate from a Maxwellian distribution.

Transition region: A very thin, nonuniform layer (a few hundred kilometers thick) in the solar atmosphere separating the chromosphere and corona. Within this region, the temperature in the solar atmosphere rises from 20,000 to over 1,000,000 degrees.

X-ray jet: A collimated jet of plasma with a temperature of a few million degrees, propelled through preexisting coronal loops, observed in X rays, and extending up to 1.5×10^5 km in length. X-ray jets are associated with small explosive flares and are thought to be produced by reconnection between emerging and existing magnetic field lines in the corona.

[70] **ACKNOWLEDGMENTS.** The authors gratefully acknowledge the contributions of the many individuals who provided programmatic and engineering support for the Solar Probe mission definition study. Special thanks are due to Ken Potocki, Doug Eng, and the APL engineering team; to Haydee Maldonado, the Solar Probe study lead, and to Chris St. Cyr, LWS Senior Scientist, both at the Goddard Space Flight Center; and to Lika Guhathakurta, the LWS Program Scientist at NASA Headquarters. Thanks also to Cesar Carrasco (University of Texas at El Paso), Justin Edmonson (University of Michigan), Stuart Bale (University of California), Bill Kurth (University of Iowa), Scott Weidner (SwRI), and Celeste Satter (JPL) for their help with a variety of technical issues. Thanks also to Rob Ebert (SwRI) for help in preparing the glossary.

[71] The Editor responsible for this paper was Peter Riley. He thanks Nathan Schwadron and an anonymous technical reviewer and one anonymous cross-disciplinary reviewer.

REFERENCES

Altschuler, M. D., and G. Newkirk Jr. (1969), Magnetic fields and the structure of the solar corona. 1: Methods of calculating coronal fields, *Sol. Phys.*, *9*, 131.

Ambrosiano, J., et al. (1988), Test particle acceleration in turbulent reconnecting magnetic fields, *J. Geophys. Res.*, *93*, 14,383.

Axford, W. I., and J. McKenzie (1992), The origin of high speed solar wind streams, in *Solar Wind Seven*, edited by E. Marsch and R. Schwenn, p. 1, Elsevier, New York.

Balogh, A., R. G. Marsden, and E. J. Smith (2001), The heliosphere and the Ulysses mission, in: *The Heliosphere Near Solar Minimum: The Ulysses Perspective*, p. 1, edited by A. Balogh, R. G. Marsden, and E. J. Smith, Springer, New York.

Biermann, L. (1951), Kometenschweife und solare Korpuskularstrahlung, *Z. Astrophys.*, *29*, 274.

Billings, D. E. (1959), Distribution of matter with temperature in the emission corona, *Astrophys. J.*, *130*, 961.

Burlaga, L. F., and K. W. Ogilvie (1970), Magnetic and thermal pressures in the solar wind, *Sol. Phys.*, *15*, 61.

Burns, J. A., P. L. Lamy, and S. Soter (1979), Radiation forces on small particles in the solar system, *Icarus*, *40*, 1.

Canals, A., et al. (2002), Estimating random transverse velocities in the fast solar wind from EISCAT interplanetary scintillation measurements, *Ann. Geophys.*, *20*, 1265.

Cane, H. V., et al. (2003), Two components in major solar particle events, *Geophys. Res. Lett.*, *30*(12), 8017, doi:10.1029/2002GL016580.

Cargill, P. J., and J. A. Klimchuk (2004), Nanoflare heating of the corona revisited, *Astrophys. J.*, *605*, 911.

Chae, J., U. Schühle, and P. Lemaire (1998), SUMER Measurements of nonthermal motions: Constraints on coronal heating mechanisms, *Astrophys. J.*, *505*, 957.

Chae, J., A. I. Poland, and M. J. Aschwanden (2002), Coronal loops heated by magnetohydrodynamic turbulence. I. A model of isobaric quiet-sun loops with constant cross sections, *Astrophys. J.*, *581*, 726.

Cliver, E. W., et al. (2004), Coronal shocks and solar energetic proton events, *Astrophys. J.*, *605*, 902.

Cohen, C. M. S., et al. (1999), New observations of heavy-ion-rich solar particle events from ACE, *Geophys. Res. Lett.*, *26*, 2697.

Coles, W. A., et al. (1991), Comparison of solar wind velocity measurements with a theoretical acceleration model, *J. Geophys. Res.*, *96*, 13,849.

Cranmer, S. R., and A. A. van Ballegooijen (2005), On the generation, propagation, and reflection of Alfvén waves from the solar photosphere to the distant heliosphere, *Astrophys. J. Suppl.*, *156*, 265.

Crooker, N. U., et al. (2004), Heliospheric plasma sheets, *J. Geophys. Res.*, *109*, A03107, doi:10.1029/2003JA010170.

Cummings, A. C., E. C. Stone, and C. D. Steenberg (2002), Composition of anomalous cosmic rays and other heliospheric ions, *Astrophys. J.*, *578*, 194.

Dalla, S., et al. (2002), Observation of decay phases of solar energetic particle events at 1 and 5 AU from the Sun, *J. Geophys. Res.*, *107*(A11), 1370, doi:10.1029/2001JA009155.

DeForest, C. E., and J. B. Gurman (1998), Observation of quasi-periodic compressive waves in solar polar plumes, *Astrophys. J.*, *501*, L217.

DeForest, C. E., et al. (2001), Observation of polar plumes at high solar altitudes, *Astrophys. J.*, *546*, 569.

Del Zanna, G., D. Chiuderi, and S. Parenti (2004), SOHO CDS and SUMER observations of quiescent filaments and their interpretation, *Astron. Astrophys.*, *420*, 307.

Domingo, V., B. Fleck, and A. I. Poland (1995), The SOHO mission: An overview, *Sol. Phys.*, *162*, 1.

Einaudi, G., et al. (1999), Formation of the slow solar wind in a coronal streamer, *J. Geophys. Res.*, *104*, 521.

Endeve, E., et al. (2005), Release of helium from closed-field regions of the Sun, *Astrophys. J.*, *624*, 402.

Feldman, W. C., et al. (1974), Interpenetrating solar wind streams, *Rev. Geophys.*, *12*, 715.

Feldman, W. C., et al. (1996), Constraints on high-speed solar wind structure near its coronal base: A ULYSSES perspective, *Astron. Astrophys.*, *316*, 355.

Feldman, W. C., et al. (1997), Experimental constraints on pulsed and steady state models of the solar wind near the Sun, *J. Geophys. Res.*, *102*, 26,905.

Fisk, L. A. (1996), Motion of the footpoints of heliospheric magnetic field lines at the Sun: Implications for recurrent energetic particle events at high heliographic latitudes, *J. Geophys. Res.*, *101*, 15,547.

Fisk, L. A. (2003), Acceleration of the solar wind as a result of the reconnection of open magnetic flux with coronal loops, *J. Geophys. Res.*, *108*(A4), 1157, doi:10.1029/2002JA009284.

Fisk, L. A., and N. A. Schwadron (2001), Origin of the solar wind: Theory, *Space Sci. Rev.*, *97*, 221.

Gabriel, A. H., F. Bely-Dubau, and P. Lemaire (2003), The contribution of polar plumes to the fast solar wind, *Astrophys. J.*, *589*, 623.

Galinsky, V. L., and V. I. Shevchenko (2000), Nonlinear cyclotron resonant wave-particle interaction in a nonuniform magnetic field, *Phys. Rev. Lett.*, *85*, 90.

Geiss, J., G. Gloeckler, and R. von Steiger (1995), Origin of the solar wind from composition data, *Space Sci. Rev.*, *72*, 49.

Georgoulis, M. K., M. Velli, and G. Einaudi (1998), Statistical properties of magnetic activity in the solar corona, *Astrophys. J.*, *497*, 957.

Gloeckler, G., et al. (2000), Sources, injection, and acceleration of heliospheric ion populations, in: *Acceleration and Transport of Energetic Particles Observed in the Heliosphere*, *AIP Conf. Proc.*, *528*, 221.

Gloeckler, G., T. H. Zurbuchen, and J. Geiss (2003), Implications of the observed anticorrelation between solar wind speed and coronal electron temperature, *J. Geophys. Res.*, *108*(A4), 1158, doi:10.1029/2002JA009286.

Goldstein, B. E., et al. (2000), Observed constraint on proton-proton relative velocities in the solar wind, *Geophys. Res. Lett.*, *27*, 53.

Golub, L., et al. (1974), Solar x-ray bright points, *Astrophys. J.*, *189*, L93.

Gopalswamy, N., et al. (2001), Near-Sun and near-Earth manifestations of solar eruptions, *J. Geophys. Res.*, *106*, 25,261.

Gopalswamy, N., et al. (2002), Interacting coronal mass ejections and solar energetic particles, *Astrophys. J.*, *572*, L103.
Gopalswamy, N., et al. (2004), Intensity variation of large solar energetic particle events associated with coronal mass ejections, *J. Geophys. Res.*, *109*, A12105, doi:10.1029/2004JA010602.
Gosling, J. T., et al. (1974), Mass ejections from the Sun: A view from SKYLAB, *J. Geophys. Res.*, *79*, 4581.
Grall, R. R., et al. (1996), Rapid acceleration of the polar solar wind, *Nature*, *379*, 429.
Grappin, R., A. Mangeney, and E. Marsch (1990), On the origin of solar wind MHD turbulence: HELIOS data revisited, *J. Geophys. Res.*, *95*, 8197.
Grün, E., et al. (1985), Collisional balance of the meteoritic complex, *Icarus*, *62*, 244.
Habbal, S. R., et al. (1997), Origins of the slow and the ubiquitous fast solar wind, *Astrophys. J.*, *489*, L103.
Haggerty, D. K., and E. C. Roelof (2002), Impulsive near-relativistic solar electron events: Delayed injection with respect to solar electromagnetic emission, *Astrophys. J.*, *579*, 841.
Hansteen, V. H., E. Leer, and T. E. Holzer (1997), The role of helium in the outer solar atmosphere, *Astrophys. J.*, *482*, 498.
Hassler, D. M., et al. (1999), Solar wind outflow and the chromospheric magnetic network, *Science*, *283*, 810.
Heyvaerts, J., and E. R. Priest (1983), Coronal heating by phase-mixed shear Alfven waves, *Astron. Astrophys.*, *117*, 220.
Hollweg, J. V., and P. A. Isenberg (2002), Generation of the fast solar wind: A review with emphasis on the resonant cyclotron interaction, *J. Geophys. Res.*, *107*(A7), 1147, doi:10.1029/2001JA000270.
Ionson, J. A. (1978), Resonant absorption of Alfvenic surface waves and the heating of solar coronal loops, *Astrophys. J.*, *226*, 650.
Isenberg, P. A. (2004), The kinetic shell model of coronal heating and acceleration by ion cyclotron waves: 3. The proton halo and dispersive waves, *J. Geophys. Res.*, *109*, A03101, doi:10.1029/2002JA009449.
Ishimoto, H. (2000), Modeling the number density distribution of interplanetary dust on the ecliptic plane within 5AU of the Sun, *Astron. Astrophys.*, *362*, 1158.
Jackson, B. V., et al. (2004), The Solar Mass-Ejection Imager (SMEI) mission, *Sol. Phys.*, *225*, 177.
Jokipii, J. R., and J. Kota (1989), The polar heliospheric magnetic field, *Geophys. Res. Lett.*, *16*, 1.
Jones, G. H., et al. (2003), Strong interplanetary field enhancements at Ulysses—Evidence of dust trails' interaction with the solar wind?, *Icarus*, *166*, 297.
Kahler, S. W. (1994), Injection profiles of solar energetic particles as funcitons of coronal mass ejection heights, *Astrophys. J.*, *428*, 837.
Kahler, S. W. (2001), The correlation between solar energetic particle peak intensities and the speeds of coronal mass ejections: Effects of ambient particle densities and energy spectra, *J. Geophys. Res.*, *106*, 20,947.
Kahler, S. W., and D. V. Reames (2003), Solar energetic particle production by coronal mass ejection-driven shocks in solar fast-wind regions, *Astrophys. J.*, *584*, 1063.
Kohl, J. L., et al. (1998), UVCS/SOHO empirical determinations of the anisotropic velocity distributions in the solar corona, *Astrophys. J.*, *501*, L127.
Krucker, S., and R. P. Lin (2000), Two classes of solar proton events dervied from onset time analysis, *Astrophys. J.*, *542*, L61.
Krucker, S., et al. (2002), Hard x-ray microflares down to 3 keV, *Sol. Phys.*, *210*, 445.
Leamon, R. J., et al. (1998), Contribution of cyclotron-resonant damping to kinetic dissipation of interplanetary Turbulence, *Astrophys. J.*, *507*, L181.
Le Roux, J. A., G. P. Zank, and W. H. Matthaeus (2002), Pickup ion acceleration by turbulent field-aligned electric fields in the slow low-latitude solar wind, *J. Geophys. Res.*, *107*(A7), 1138, doi:10.1029/2001JA000285.
Levine, R. H. (1978), The relation of open magnetic structures to solar wind flow, *J. Geophys. Res.*, *83*, 4193.
Li, G., and G. P. Zank (2005), Mixed particle acceleration at CME-driven shocks and flares, *Geophys. Res. Lett.*, *32*, L02101, doi:10.1029/2004GL021250.
Li, X., et al. (1998), The effect of temperature anisotropy on obsevations of Doppler dimming and pumping in the inner corona, *Astrophys. J.*, *501*, L133.
Liewer, P. C., M. Neugebauer, and T. Zurbuchen (2004), Characteristics of active-region sources of solar wind near solar maximum, *Sol. Phys.*, *223*, 209.
Longcope, D. W., D. S. Brown, and E. R. Priest (2003), On the distribution of magnetic null points above the solar photosphere, *Phys. Plasmas*, *10*, 3321.
Mann, I., and A. Czechowski (2005), Dust destruction and ion formation in the inner solar system, *Astrophys. J.*, *621*, L73.
Mann, I., A. Krivov, and H. Kimura (2000), Dust cloud near the Sun, *Icarus*, *146*, 568.
Mann, I., et al. (2004), Dust near the Sun, *Space Sci. Rev.*, *110*, 269.
Mann, I., et al. (2005), Physical properties of the dust in the solar system and its interrelation with small bodies, in *Asteroids, Comets, Meteors*, *Proc. IAU Symp.*, vol. 299, edited by D. Lazzaro, S. Ferraz-Mello, and J. A. Fernández, p. 41, Cambridge Univ. Press, New York.
Marsch, E., and C.-Y. Tu (2001), Heating and acceleration of coronal ions interacting with plasma waves through cyclotron and Landau resonance, *J. Geophys. Res.*, *106*, 227.
Marsch, E., et al. (1982), Solar wind protons: Three-dimensional velocity distributions and derived plasma parameters measured between 0.3 and 1 AU, *J. Geophys. Res.*, *87*, 52.
Mason, G. M., et al. (1989), Impulsive acceleration and scatter-free transport of $\sim$1 MeV per nucleon ions in 3He-rich solar particle events, *Astrophys. J.*, *339*, 529.
Mason, G. M., et al. (1999), ^{3}He enhancements in large solar energetic particle events, *Astrophys. J.*, *525*, L133.
Mason, G. M., et al. (2004), Abundances of heavy and ultraheavy ions in ^{3}He-rich solar flares, *Astrophys. J.*, *606*, 555.
Matthaeus, W. H., and M. L. Goldstein (1986), Low-frequency 1/f noise in the interplanetary magnetic field, *Phys. Rev. Lett.*, *57*, 495.
Matthaeus, W. H., and S. L. Lamkin (1986), Turbulent magnetic reconnection, *Phys. Fluids*, *29*, 2513.
Matthaeus, W. H., et al. (1999), Coronal heating by magnetohydrodynamic turbulence driven by reflected low-frequency waves, *Astrophys. J.*, *523*, L93.
McComas, D. J., et al. (2001), Ulysses' second orbit: Remarkably different solar wind, *Space Sci. Rev.*, *97*, 99.
McComas, D. J., et al. (2003), The three-dimensional solar wind around solar maximum, *Geophys. Res. Lett.*, *30*(10), 1517, doi:10.1029/2003GL017136.
McKenzie, D. E., and D. J. Mullan (1997), Periodic modulation of x-ray intensity from coronal loops: Heating by resonant absorption, *Sol. Phys.*, *176*, 127.
McKibben, R. B., C. Lopate, and M. Zhang (2001), Simultaneous observations of solar energetic particle events by IMP 8 and the Ulysses Cospin High Energy Telescope at high solar latitudes, *Space Sci. Rev.*, *97*, 257.
Mewaldt, R. A., et al. (2003), Heavy ion and electron releases time in solar particle events, *Proc. Int. Conf. Cosmic Rays 28th*, 3313.
Miller, J. A. (1998), Particle acceleration in impulsive solar flares, *Space Sci. Rev.*, *86*, 79.
Misconi, N. Y. (1993), The spin of cosmic dust: Rotational bursting of circumsolar dust in the *F* corona, *J. Geophys. Res.*, *98*, 18,951.
Murphy, N., E. J. Smith, and N. A. Schwadron (2002), Strongly underwound magnetic fields in co-rotating interaction regions: Observations and implications, *Geophys. Res. Lett.*, *29*(22), 2066, doi:10.1029/2002GL015164.
Narain, U., and P. Ulmschneider (1996), Chromospheric and coronal heating mechanisms II, *Space Sci. Rev.*, *75*, 453.

NASA (2005a), Solar Probe: Report of the Science and Technology Definition Team, *NASA Tech. Memo., TM-2005-212786*.
NASA (2005b), Sun-solar system connection: Science and technology roadmap 2005–2035, report, 127 pp., Greenbelt, Md. (Available at http://sec.gsfc.nasa.gov/SSSC_2005Roadmap.pdf)
National Research Council (2003), *The Sun to the Earth—And Beyond: A Decadal Research Strategy in Solar and Space Physics*, Natl. Acad. of Sci., Washington, D. C.
Neugebauer, M. (1991), The quasi-stationary and transient states of the solar wind, *Science*, *252*, 404.
Neugebauer, M., et al. (1995), Ulysses observations of microstreams in the solar wind from coronal holes, *J. Geophys. Res.*, *100*, 23,389.
Neugebauer, M., et al. (2002), Sources of the solar wind at solar activity maximum, *J. Geophys. Res.*, *107*(A12), 1488, doi:10.1029/2001JA000306.
Noci, G. (2002), The temperature of the solar corona, *Mem. Soc. Astron. Ital.*, *74*, 704.
Noci, G., et al. (1997), First results from UVCS/SOHO, *Adv. Space Res.*, *20*(12), 2219.
Ofman, L. (2000), Source regions of the slow solar wind in coronal structures, *Geophys. Res. Lett.*, *27*, 2885.
Ofman, L. (2005), MHD waves and heating in coronal holes, *Space Sci. Rev.*, *120*, 67.
Ofman, L., et al. (1997), Ultraviolet Coronagraph Spectrometer observations of density fluctuations in the solar wind, *Astrophys. J.*, *491*, L111.
Ofman, L., V. M. Nakariakov, and C. E. DeForest (1999), Slow magnetosonic waves in coronal plumes, *Astrophys. J.*, *514*, 441.
Ofman, L., et al. (2000), UVCS WLC observations of compressional waves in the south polar coronal hole, *Astrophys. J.*, *529*, 592.
Ofman, L., S. P. Gary, and A. Viñas (2002), Resonant heating and acceleration of ions in coronal holes driven by cyclotron resonant spectra, *J. Geophys. Res.*, *107*(A12), 1461, doi:10.1029/2002JA009432.
Ogawara, Y., et al. (1991), The Solar-A mission: An overview, *Sol. Phys.*, *136*, 1.
Ogilvie, K. W., and M. D. Desch (1997), The WIND spacecraft and its early scientific results, in *Results of the IASTP Program*, edited by C. T. Russell, p. 559, Elsevier, New York.
Parker, E. N. (1958), Dynamics of the interplanetary gas and magnetic fields, *Astrophys. J.*, *128*, 644.
Parker, E. N. (1988), Nanoflares and the solar x-ray corona, *Astrophys. J.*, *330*, 474.
Parker, E. N. (1997), Mass ejection and a brief history of the solar wind concept, in *Cosmic Winds and the Heliosphere*, edited by J. R. Jokipii, C. P. Sonett, and M. S. Giampapa, p. 3, Univ. of Ariz. Press, Tucson.
Paularena, K. I., and J. H. King (1999), NASA's IMP 8 spacecraft, in *Interball in the ISTP Program: Studies of the Solar Wind-Magnetosphere-Ionosphere Interaction*, edited by D. G. Sibeck and K. Kudela, p. 145, Springer, New York.
Ragot, B. R., and S. W. Kahler (2003), Interactions of dust grains with coronal mass ejections and solar cycle variations of the *F*-corona brightness, *Astrophys. J.*, *594*, 1049.
Rappazzo, A. F., M. Velli, G. Einaudi, and R. B. Dahlburg (2005), Diamagnetic and expansion effects on the observable properties of the slow solar wind in a coronal streamer, *Astrophys. J.*, *633*, 474.
Raymond, J. C., et al. (1998), Solar wind at 6.8 solar radii from UVCS observation of comet C/19 96Y1, *Astrophys. J.*, *508*, 410.
Reames, D. V. (1999), Particle acceleration in the Sun and the heliosphere, *Space Sci. Rev.*, *90*, 413.
Reames, D. V., and C. K. Ng (2004), Heavy-element abundances in solar energetic particle events, *Astrophys. J.*, *610*, 510–522.
Schatten, K. H., J. M. Wilcox, and N. F. Ness (1969), A model of interplanetary and coronal magnetic fields, *Sol. Phys.*, *6*, 442.
Schrijver, C. J., et al. (1997), Sustaining the quiet photospheric network: The balance of flux emergence, fragmentation, merging, and cancellation, *Astrophys. J.*, *487*, 424.
Schrijver, C. J., et al. (1998), Large-scale coronal heating by the small-scale magnetic field of the Sun, *Nature*, *394*, 152.
Schrijver, C. J., et al. (1999), A new view of the solar outer atmosphere by the Transition Region and Coronal Explorer, *Sol. Phys.*, *187*, 261.
Schwadron, N. A. (2002), An explanation for strongly underwound magnetic field in co-rotating rarefaction regions and its relationship to footpoint motion on the the sun, *Geophys. Res. Lett.*, *29*(14), 1663, doi:10.1029/2002GL015028.
Schwadron, N. A., and D. J. McComas (2003), Solar wind scaling law, *Astrophys. J.*, *599*, 1395.
Schwenn, R., and E. Marsch (Eds.) (1990), *Physics of the Inner Heliosphere*, vols. 1 and 2, Springer, New York.
Scudder, J. D. (1994), Ion and electron suprathermal tail strengths in the transition region: Support for the velocity filtration model of the corona, *Astrophys. J.*, *427*, 446.
Sheeley, N. R., Jr., et al. (1997), Measurements of Flow Speeds in the Corona between 2 and 30 R_S, *Astrophys. J.*, *484*, 472.
Sittler, E. C., and M. Guhathakurta (1999), Semiempirical two-dimensional magnetohydrodynamic model of the colar corona and interplanetary medium, *Astrophys. J.*, *523*, 812.
Sittler, E. C., and M. Guhathakurta (2002), Erratum: "Semiempirical two-dimensional magnetohydrodynamic model of the colar corona and interplanetary medium," *Astrophys. J.*, *564*, 1062.
Smith, E. J. (2001), The heliospheric current sheet, *J. Geophys. Res.*, *106*, 15,819.
Smith, E. J., et al. (2003), The Sun and heliosphere at solar maximum, *Science*, *302*, 1165.
Sokolov, I. V., et al. (2004), A new field line advection model for solar particle acceleration, *Astrophys. J.*, *616*, L171.
Sterling, A. C. (2000), Solar spicules: A review of recent models and targets for future observations, *Sol. Phys.*, *196*, 79.
Stone, E. C., et al. (1998), The Advanced Composition Explorer, *Space Sci. Rev.*, *86*, 1.
Teriaca, L., et al. (2003), The nascent solar wind: Origin and acceleration, *Astrophys. J.*, *688*, 566.
Thieme, K. M., R. Schwenn, and E. Marsch (1989), Are structures in high-speed streams signatures of coronal fine structures?, *Adv. Space Res.*, *9*(4), 127.
Thomson, D. J., C. G. Maclennan, and L. J. Lanzerotti (1995), Propagation of solar oscillations through the interplanetary medium, *Nature*, *376*, 139.
Tsurutani, B. T., et al. (2002), Phase-steepend Alfvén waves, proton perpendicular energization, and the creation of magnetic holes and magnetic decreases: The ponderomotive force, *Geophys. Res. Lett.*, *29*(24), 2233, doi:10.1029/2002GL015652.
Tu, C.-Y., E. Marsch, and Z.-R. Qin (2004), Dependence of the proton beam drift velocity on the proton core plasma beta in the solar wind, *J. Geophys. Res.*, *109*, A05101, doi:10.1029/2004JA010391.
Tu, C.-Y., et al. (2005), Solar wind origin in coronal funnels, *Science*, *308*, 519.
Tylka, A. J., et al. (2005), Shock geometry, seed populations, and the origin of variable elemental composition at high energies in large gradual solar particle events, *Astrophys. J.*, *625*, 474.
Uchida, Y., et al. (1992), Continual expansion of the active-region corona observed by the Yohkoh soft X-ray telescope, *Publ. Astron. Soc. Jpn.*, *44*, L155.
Velli, M. (1993), On the propagation of ideal, linear Alfvén waves in radially stratified stellar atmospheres and winds, *Astron. Astrophys.*, *270*, 304.
Wang, Y.-M., and N. R. Sheeley Jr. (1990), Solar wind speed and coronal flux-tube expansion, *Astrophys. J.*, *355*, 726.
Wang, Y.-M., et al. (1997), Solar wind stream interactions and the wind speed-expansion factor relationship, *Astrophys. J.*, *488*, L51.
Wilhelm, K., et al. (1998), The solar corona above polar coronal holes as seen by SUMER on SOHO, *Astrophys. J.*, *500*, 1023.

Withbroe, G. L., and R. W. Noyes (1977), Mass and energy flow in the solar chromosphere and corona, *Annu. Rev. Astron. Astrophys.*, *15*, 363.

Yamauchi, Y., et al. (2004), The magnetic structure of Hα macrospicules in solar coronal holes, *Astrophys. J.*, *605*, 511.

Zank, G. P., et al. (2000), Particle acceleration and coronal mass ejection driven shocks: A theoretical model, *J. Geophys. Res.*, *105*, 25,079.

Zhang, M., and B. C. Low (2005), The hydromagnetic nature of solar coronal mass ejections, *Annu. Rev. Astron. Astrophys.*, *43*, 103.

Zurbuchen, T. H., et al. (2002), The solar wind composition throughout the solar cycle: A continuum of dynamic states, *Geophys. Res. Lett.*, *29*(9), 1352, doi:10.1029/2001GL013946.

L. W. Acton, Department of Physics, Montana State University, P.O. BOX 173840, Bozeman, MT 59717-3840, USA.

M. Balat-Pichelin, PROMES-CNRS, B.P. 5 Odeillo, F-66125 Font Romeu Cedex, France.

V. Bothmer, Institut für Astrophysik, Georg-August-Universität Göttingen, D-37077 Göttingen, Germany.

R. B. Dirling Jr., SAIC, 17330 Brookhurst Street, Fountain Valley, CA 92708, USA.

W. C. Feldman, Los Alamos National Laboratory, Los Alamos, NM 87545, USA.

G. Gloeckler, Department of Physics, University of Maryland, College Park, MD 20742, USA.

S. R. Habbal, Institute for Astronomy, University of Hawaii at Manoa, 2680 Woodlawn Drive, Honolulu, HI 96822, USA.

D. M. Hassler, Southwest Research Institute, Suite 400, Boulder, CO 80302, USA.

W. S. Lewis and D. J. McComas, Space Science and Engineering Division, Southwest Research Institute, P.O. Drawer 28510, San Antonio, TX 78228-0510, USA. (dmccomas@swri.edu)

I. Mann, Department of Earth and Planetary Sciences, Kobe University, Nada, Kobe 657-8501, Japan.

W. H. Matthaeus, Bartol Research Institute, University of Delaware, Newark, DE 19716, USA.

R. L. McNutt Jr., Johns Hopkins University Applied Physics Laboratory, Rm MP3-E116, 11100 Johns Hopkins Road, Laurel, MD 20723, USA.

R. A. Mewaldt, Space Radiation Laboratory, California Institute of Technology, 220-47, Pasadena, CA 91125, USA.

N. Murphy, Jet Propulsion Laboratory, 4800 Oak Grove Drive, MS 169-506, Pasadena, CA 91109, USA.

L. Ofman, Physics Department, Catholic University of America, Washington, DC 20064, USA.

E. C. Sittler Jr., NASA Goddard Space Flight Center, MC 673, Greenbelt, MD 20771, USA.

C. W. Smith, Department of Earth, Oceans and Space, University of New Hampshire, 207 Morse Hall, Durham, NH 03824, USA.

M. Velli, Dipartimento di Astronomia e Scienza dello Spazio, Università degli Studi di Firenze, Largo E. Fermi 2, I-50125 Florence, Italy.

T. H. Zurbuchen, Department of Atmospheric, Oceanic, and Space Science, University of Michigan, 2455 Hayward Street, Ann Arbor, MI 48109, USA.